STATISTICS, OPTIMIZATION AND INFORMATION COMPUTING
*Stat., Optim. Inf. Comput.*, Vol. **14**, July 2025, pp 77–104.
Published online in International Academic Press (www.IAPress.org)

# The New Topp-Leone-Marshall-Olkin-Gompertz-G Family of Distributions: Properties, Different Estimation Techniques and Applications on Censored and Complete Data

Peter T. Chinofunga [1,2,*], Broderick Oluyede [2], Fastel Chipepa [2]

[1] *Department of Mathematics and Computer Science, Great Zimbabwe University, Zimbabwe*
[2] *Department of Mathematics and Statistical Sciences, Botswana International University of Science and Technology, Botswana*

**Abstract** A new family of distributions (FoD) called the Topp-Leone-Marshall-Olkin Gompertz-G is presented in this paper. Derivations of some statistical properties were carried out. The model parameters were estimated using five methods, including weighted least squares, maximum likelihood estimation, least squares, Cramér-von Mises, and Anderson Darling. The simulation experiment assessed the precision of the model parameters through the utilization of five estimation methods. To evaluate the adaptability and utility of this new FoD, three real-life datasets were analyzed using a special case from the developed family of distributions, one of which contained censored data. Remarkably, the new model showed exceptional performance when compared against six other non-nested models. This comparison highlighted its superiority and effectiveness in modeling real-life datasets.

**Keywords** Gompertz-G distribution, Marshall-Olkin-G distribution, maximum likelihood estimation, least squares, weighted least squares, Anderson Darling, Cramér-von Mises, likelihood ratio test.

**AMS 2010 subject classifications** 62E30; 60E05; 62E15

**DOI:** 10.19139/soic-2310-5070-2239

## 1. Introduction

The past two decades have witnessed a substantial rise in the demand for generalized distributions due to their ability to effectively handle skewness and kurtosis. While generalized distributions offer enhanced flexibility and versatility, there are scenarios where classical distributions may outperform them. Some key situations where classical distributions may be preferred are

- When the dataset is small, classical distributions with fewer parameters (e.g., exponential, Weibull, or normal distributions) tend to perform better.
- In fields where distribution interpretability is critical (for example, healthcare, finance, or engineering), classical distributions are often preferred.
- When computational resources are limited or when real-time analysis is required, classical distributions are advantageous.
- When the underlying data exhibits simple patterns (e.g., constant hazard rates, symmetric distributions, or light-tailed behaviour), classical distributions may suffice.
- In situations where the true data-generating process is unknown or partially known, classical distributions may be more robust.

*Correspondence to: Peter Tinashe Chinofunga (Email:ptchinofunga@gzu.ac.zw). Department of Mathematics and Computer Science, Great Zimbabwe University, Zimbabwe.

ISSN 2310-5070 (online) ISSN 2311-004X (print)

- In applications where quick implementation is required, classical distributions are often preferred.
- When the analysis focuses on specific features of the data (e.g., mean, variance, or tail behaviour), classical distributions tailored to those features may outperform generalized distributions.
- In regulated industries (e.g., pharmaceuticals, finance), classical distributions may be required to comply with industry standards or regulatory guidelines.
- When the dataset contains noise or outliers, classical distributions may generalize better to new data.
- In teaching or introductory courses, classical distributions are often used to illustrate fundamental concepts.

However, the surge in demand for generalized distributions can be linked to the recognition of their efficacy in addressing skewness and kurtosis traits in data analysis. The applications of generalized distributions span diverse domains such as finance, economics, hydrology, physics, reliability, and engineering. Several authors, including Cordeiro et al. [15], Zografos and Balakrishnan [40], Cleaton and Lynch [14], Alizadeh et al. [5], have demonstrated the effectiveness of numerous generators in generalizing classical distributions. Also, Nasiru and Abubakari [29], Opone and Osemwenkhae [32], Abdullah et al. [1], Alsultan [6], Ehiwario et al. [17], Osi et al. [33], Atchadé et al. [7] and Nkomo et al. [30], among others, have contributed to the validation and exploration of these generators, demonstrating their use in extending the scope of classical distributions.

One distribution whose application covers areas such as income, reliability, actuarial science and medical science is the Gompertz distribution. Some of the available literature on the generalisation of this distribution includes work by Oluyede et al. [31], Chipepa and Oluyede [13], El-Gohary et al. [18], Codeiro et al. [16], and Jafari et al. [21]. The cumulative distribution function (cdf) and the probability density function (pdf) of the Gompertz-G (Gom-G) family of distributions (FoD) as given by Alizadeh et al. [5] are

$$F_{Gom-G}(z;\theta,\gamma,\Psi)=1-e^{\frac{\theta}{\gamma}\left(1-\left[\bar{G}(z;\Psi)\right]^{-\gamma}\right)} \tag{1}$$

and

$$f_{Gom-G}(z;\theta,\gamma,\Psi)=\theta g(z;\Psi)\left[\bar{G}(z;\Psi)\right]^{-\gamma-1}e^{\frac{\theta}{\gamma}\left(1-\left[\bar{G}(z;\Psi)\right]^{-\gamma}\right)} \tag{2}$$

for $\gamma,\theta>0$, where $\bar{G}(z;\Psi)$ is the baseline distribution depending on parameter vector $\Psi$ and $\bar{G}(z;\Psi)=1-G(z;\Psi)$.

The primary purpose of this research is to generalise the Gom-G distribution, using the combined generator Topp-Leone-Marshall-Olkin-G (TLMOG) FoD by Chipepa et al. [12], culminating in the new Topp-Leone-Marshall-Olkin-Gompertz-G (TLMOGom-G) FoD. The TLMO-G FoD cdf is

$$F_{TLMO-G}(z;b,\delta,\Psi)=\left[1-\frac{\delta^2\bar{G}^2(z;\Psi)}{\left(1-\bar{\delta}\bar{G}(z;\Psi)\right)^2}\right]^b \tag{3}$$

for $\delta,b>0$ and $\bar{\delta}=1-\delta$. The hazard rate functions (hrf) of the TLMO-G distribution can exhibit both monotonic and non-monotonic shapes, as demonstrated in the study on the Topp-Leone-Marshall-Olkin-loglogistic special model by Chipepa et al. [12].

The motivations behind the development of the TLMOGom-G FoD are:

- Current distributions often lack the ability to simultaneously capture monotonic, non-monotonic, and heavy-tailed hazard rate shapes. These properties are crucial for accurately modeling real-world phenomena, where diverse failure rates and risk patterns are frequently observed. Enhancing the flexibility of hazard rate functions is essential for improving the precision of statistical models in practical applications.

- Some generalized distributions fail to adequately model heavy-tailed data, despite the importance of such distributions in representing extreme events. This limitation hinders their applicability in scenarios where extreme values or rare events are prevalent.
- Some existing distributions lack the versatility to model datasets exhibiting both skewed and symmetrical characteristics. This restricts their utility across a wide range of real-world data, which often display varying degrees of skewness and symmetry.
- There is a pressing need to develop new generalized distribution models that offer superior fit and flexibility compared to existing ones. Such advancements would address the limitations of current models and provide more robust tools for statistical analysis.

Thus, the primary objectives of this study are as follows:

- To introduce and derive the TLMOGom-G FoD.
- To derive and analyze the key mathematical and statistical properties of the TLMOGom-G FoD.
- To demonstrate the flexibility of the TLMOGom-G FoD in modeling diverse types of data.
- To look for the best estimation technique for parameter estimation of the TLMOGom-G FoD.
- To conduct simulation studies to evaluate the consistency and reliability of the parameter estimates derived from the TLMOGom-G FoD.
- To compare the performance of the TLMOGom-G FoD with other competing equi-parameter models to demonstrate its superiority in terms of fit and applicability.
- To compare the performance of the TLMOGom-G FoD with some nested models.

The outline of this paper is: Section 2 presents the model and the associated properties. Section 3 looks at estimation of the parameters. Special cases of the new family are presented in Section 4. Section 5 looks at simulation studies. Applications are dealt with in Section 6 and the summary is contained in Section 7.

## 2. The Model

The TLMOGom-G FoD and its statistical properties are developed under this section. Employing equations (1.1) and (1.3), setting $\theta = 1$ to avoid over-parameterization (see model identifiability) and letting $h(z;\gamma,\Psi) = \frac{1}{\gamma}\left[1-\left(\bar{G}(z;\Psi)\right)^{-\gamma}\right]$, the cdf, pdf and hrf, respectively, of the TLMOGom-G FoD are:

$$F_{TLMOGom-G}(z;\delta,b,\gamma,\Psi) = \left[1-\frac{\delta^2 e^{2h(z;\Psi)}}{\left(1-(1-\delta)e^{h(z;\Psi)}\right)^2}\right]^b, \tag{4}$$

$$\begin{aligned} f_{TLMOGom-G}(z;\delta,b,\gamma,\Psi) &= \frac{2b\delta^2 g(z;\Psi)\left(\bar{G}(z;\Psi)\right)^{-\gamma-1} e^{2h(z;\Psi)}}{\left(1-(1-\delta)e^{h(z;\Psi)}\right)^3} \\ &\times \left[1-\frac{\delta^2 e^{2h(z;\Psi)}}{\left(1-(1-\delta)e^{h(z;\Psi)}\right)^2}\right]^{b-1}, \end{aligned} \tag{5}$$

and

$$
\begin{aligned}
h_{TLMOGom-G}(z;\delta,b,\gamma,\Psi) &= \frac{2b\delta^2 g(z;\Psi)\left(\bar{G}(z;\Psi)\right)^{-\gamma-1} e^{2h(z;\Psi)}}{\left(1-(1-\delta)e^{h(z;\Psi)]}\right)^3} \\
&\times \left[1-\frac{\delta^2 e^{2h(z;\Psi)}}{\left(1-(1-\delta)e^{h(z;\Psi)}\right)^2}\right]^{b-1} \\
&\times \left\{1-\left[1-\frac{\delta^2 e^{2h(z;\Psi)}}{\left(1-(1-\delta)e^{h(z;\Psi)]}\right)^2}\right]^b\right\}^{-1} \qquad (6)
\end{aligned}
$$

for $\delta, b, \gamma > 0$, and a vector of parameters $\Psi$.

### *2.1. Model Identifiability*

It is a fundamental concept in statistical modelling and data analysis. Its purpose is to ensure that the parameters of a model can be uniquely determined from the observed data. Also, identifiability encourages the use of parsimonious models, which are simpler and more interpretable. We seek to demonstrate the identifiability of the TLMOGom-G FoD model.

Let $\Delta_1 = (\delta_1, b_1, \gamma_1, \Psi_1)$ and $\Delta_2 = (\delta_2, b_2, \gamma_2, \Psi_2)$, then, the likelihood ratio is

$$
\begin{aligned}
\frac{f_1(\Delta_1)}{f_2(\Delta_2)} &= \left[\frac{2b_1\delta_1^2}{2b_2\delta_2^2}\right]\left[\frac{g(z;\Psi_1)}{g(z;\Psi_2)}\right]\left[\frac{\left(\bar{G}(z;\Psi_1)\right)^{-\gamma_1-1}}{\left(\bar{G}(z;\Psi_2)\right)^{-\gamma_2-1}}\right]\left[\frac{\left(1-(1-\delta_2)e^{h(z;\Psi_2)}\right)^3}{\left(1-(1-\delta_1)e^{h(z;\Psi_1)}\right)^3}\right] \\
&\times \left[\frac{\left\{1-\frac{\delta_1^2 e^{2h(z;\Psi_1)}}{\left[1-(1-\delta_1)e^{h(z;\Psi_1)}\right]^2}\right\}^{b_1-1}}{\left\{1-\frac{\delta_2^2 e^{2h(z;\Psi_2)}}{\left[1-(1-\delta_2)e^{h(z;\Psi_2)}\right]^2}\right\}^{b_2-1}}\right] e^{h(z;\Psi_1)-h(z;\Psi_2)}.
\end{aligned}
$$

The log-likelihood ratio is

$$
\begin{aligned}
\ln\left[\frac{f_1(\Delta_1)}{f_2(\Delta_2)}\right] &= \ln\left[\frac{2b_1\delta_1^2}{2b_2\delta_2^2}\right] + \ln\left[g(z;\Psi_1)\right] - \ln\left[g(z;\Psi_2)\right] - (\gamma_1+1)\ln\left[\bar{G}(z;\Psi_1)\right] \\
&+ (\gamma_2+1)\ln\left[\bar{G}(z;\Psi_2)\right] + \ln\left[\left(1-(1-\delta_2)e^{h(z;\Psi_2)}\right)^3\right] \\
&- \ln\left[\left(1-(1-\delta_1)e^{h(z;\Psi_1)}\right)^3\right] + (b_1-1)\ln\left[1-\frac{\delta_1^2 e^{2h(z;\Psi_1)}}{\left[1-(1-\delta_1)e^{h(z;\Psi_1)}\right]^2}\right] \\
&- (b_2-1)\ln\left[1-\frac{\delta_2^2 e^{2h(z;\Psi_2)}}{\left[1-(1-\delta_2)e^{h(z;\Psi_2)}\right]^2}\right] + \left[h(z;\Psi_1)-h(z;\Psi_2)\right]. \qquad (7)
\end{aligned}
$$

Differentiating equation (7) gives

$$\begin{aligned}\frac{d\ln\left[\frac{f_1(\Delta_1)}{f_2(\Delta_2)}\right]}{dz} &= \frac{g'(z;\Psi_1)}{g(z;\Psi_1)}-\frac{g'(z;\Psi_2)}{g(z;\Psi_2)}-(\gamma_1+1)\frac{\frac{g'(z;\Psi_1)}{g(z;\Psi_1)}}{\bar{G}(z;\Psi_1)}+(\gamma_2+1)\frac{\frac{g'(z;\Psi_2)}{g(z;\Psi_2)}}{\bar{G}(z;\Psi_2)}\\ &- \frac{3(1-\delta_1)e^{h(z;\Psi_1)}h'(z;\Psi_1)}{\left(1-(1-\delta_1)e^{h(z;\Psi_1)}\right)^3}+\frac{3(1-\delta_2)e^{h(z;\Psi_2)}h'(z;\Psi_2)}{\left(1-(1-\delta_2)e^{h(z;\Psi_2)}\right)^3}\\ &+ (b_1-1)\frac{2\delta_1^2e^{2h(z;\Psi_1)}h'(z;\Psi_1)}{\left[1-(1-\delta_1)e^{h(z;\Psi_1)}\right]^3\left[1-\frac{\delta_1^2e^{2h(z;\Psi_1)}}{\left[1-(1-\delta_1)e^{h(z;\Psi_1)}\right]^2}\right]}\\ &- (b_2-1)\frac{2\delta_2^2e^{2h(z;\Psi_2)}h'(z;\Psi_2)}{\left[1-(1-\delta_2)e^{h(z;\Psi_2)}\right]^3\left[1-\frac{\delta_2^2e^{2h(z;\Psi_2)}}{\left[1-(1-\delta_2)e^{h(z;\Psi_2)}\right]^2}\right]}\\ &+ h'(z;\Psi_1)-h'(z;\Psi_2),\end{aligned}$$

When the derivative of the natural logarithm of the ratio of two functions, $\ln\left[\frac{f_1(\Delta_1)}{f_2(\Delta_2)}\right]$, with respect to z equals zero, i.e.,

$$\frac{d\ln\left[\frac{f_1(\Delta_1)}{f_2(\Delta_2)}\right]}{dz}=0,$$

it implies $\Delta_1=\Delta_2$. This equality signifies that the parameters of the TLMOGom-G FoD can be uniquely determined from a given dataset, ensuring identifiability of the model. In other words, it guarantees that the parameters of the model are uniquely identifiable, allowing for reliable estimation and interpretation of the model.

### 2.2. Quantile Function

The quantile function is obtained by computing the inverse of the cdf. Thus, the TLMOGom-G FoD's quantile values are obtained using solutions of the equation

$$Q_z(w)=G^{-1}\left[1-\left(1-\gamma ln\left(\frac{\sqrt{1-w^{\frac{1}{b}}}}{\delta+\bar{\delta}\sqrt{1-w^{\frac{1}{b}}}}\right)\right)^{-\frac{1}{\gamma}}\right],$$

for $0<w<1$. Refer to the appendix for the derivation.

### 2.3. Linear Representation

Series expansion of the TLMOGom-G FoD, useful for further derivations of the associated and necessary statistical properties is presented in this section (see **web appendix**). The linear representation is given by

$$f_{TLMOGom-G}(z;\delta,b,\gamma,\Psi)=\sum_{n=0}^{\infty}\Upsilon_{n+1}g_{n+1}(z;\Psi), \tag{8}$$

where

$$\begin{aligned}\Upsilon_{n+1} &= 2b\sum_{i,j,k,m=0}^{\infty}(-1)^i\delta^{2(i+1)}\bar{\delta}^j\frac{(2i+j+2)^k}{(n+1)\gamma^k k!}\\ &\times \binom{b-1}{i}\binom{2i+j+2}{j}\binom{\gamma+m-k}{m}\binom{m\gamma+n-1}{n}\end{aligned} \tag{9}$$

and $g_{n+1}(z;\Psi) = (n+1)g(z;\Psi)G^n(z;\Psi)$. Consequently, the TLMOGom-G FoD can be represented as an infinite linear combination of the Expon-G distributions, with power parameter $(n+1)$ and linear component $\Upsilon_{n+1}$. The properties of this FoD are derived from the underlying Expon-G distribution.

### *2.4. Distribution of Order Statistics*

Order statistics refer to the arrangement of sample values in ascending order. Consider $Z_{(1)} \leq Z_{(2)} \leq \ldots \leq Z_{(m)}$ as the order statistics from the TLMOGom-G. The pdf of the $i^{th}$ order statistic from the TLMOGom-G FoD is

$$f_{TLMOGom-G}(z;\delta,b,\gamma,\Psi)) \quad = \quad \sum_{q=0}^{\infty} \nu^*_{q+1} g_{q+1}(z;\Psi), \tag{10}$$

where $g_{q+1}(z;\Psi) = (q+1)g(z;\Psi)G^q(z;\Psi)$ is the Expon-G distribution whose power parameter is $(q+1)$, and

$$\begin{aligned} \nu^*_{q+1} \quad &= \quad 2b\delta^{2k+1}\bar{\delta}^l \sum_{k,l,n,p=0}^{\infty} \sum_{j=0}^{m-j} (-1)^{k+p} \frac{(2k+l+1)^n}{(q+1)B(i;m-i+1)n!} \left(\frac{1}{\gamma}\right)^n \\ &\times \quad \binom{m-i}{j}\binom{b(j+i)-1}{k}\binom{2k+l+2}{l}\binom{n}{p}\binom{\gamma(p+1)+q}{q} \end{aligned} \tag{11}$$

is the linear component. Refer to the **web appendix** for details.

### *2.5. Entropy*

An entropy quantifies the level of randomness or uncertainty within a system. Rényi entropy, introduced by Rényi [34], extends the concept of Shannon entropy, first proposed by Shannon [37]. The TLMOGom-G FoD Rényi entropy (refer to the appendix for its derivation) is given by

$$I_R(a) = (1-a)^{-1} \log \left[ \sum_{n=0}^{\infty} K_n \exp[(1-a)I_{REG}] \right], \tag{12}$$

where

$$\begin{aligned} K_n \quad &= \quad (2b)^a \sum_{i,j,k,m=0}^{\infty} (-1)^{i+m} \delta^{2(a+i)} \frac{(j+a)^k}{k!\gamma^k} \binom{a(b-1)}{i} \\ &\times \quad \binom{2i+3a+j-1}{j}\binom{k}{m}\binom{\gamma(m+a)+a+n-1}{n}\left(\frac{1}{\frac{n}{a}+1}\right)^a \end{aligned}$$

and

$$I_{REG} = \int_0^{\infty} \left[ \left(\frac{n}{a}+1\right) g(z;\Psi) G^{\frac{n}{a}}(z;\Psi) \right]^a dz$$

is the Rényi entropy of the Expon-G density with power parameter $\left(\frac{n}{a}+1\right)$. Details of the derivations are in the **web appendix**.

### *2.6. Stochastic Ordering*

Stochastic ordering provides a statistical framework to compare random variables and determine if one variable is stochastically smaller than another. Simply put, a stochastic order is comparison of two random variables to see if one is generally ”larger” or ”smaller” than the other. However, it may not be easy to pick it up with a naked eye. Sometimes, two random variables can’t be clearly ranked as one being larger, smaller, or equal to the other.

There are different types of these comparisons, each useful for specific situations. It is very useful in such areas as hypothesis testing, simultaneous comparisons, multiple decisions problems and decisions under risk.

Now, consider two random variables, $Z$ and $W$. The cdf of $Z$ is denoted by $F_Z(t)$ and that of $W$ by $F_W(t)$. Similarly, the survival functions are denoted by $\bar{F}_Z(t) = 1 - F_Z(t)$ and $\bar{F}_W(t) = 1 - F_W(t)$, respectively. $Z$ is stochastically smaller than $W$ if either $F_Z(t) \geq F_W(t)$ or $\bar{F}_Z(t) \leq \bar{F}_W(t)$ for all values of $t$ in the real number space. This relationship is represented as $Z <_{so} W$. To establish that $Z$ and $W$ are stochastically ordered, we utilize other stochastic orders, such as the hazard rate order (hro) and the likelihood ratio order (lro). Based on the work by Shaked and Shanthikumar [35], it is known that if $Z <_{lro} W$, indicating that $Z$ is stochastically smaller than $W$ according to the likelihood ratio order, then it follows that $Z <_{hro} W$, signifying the hazard rate order, and consequently $Z <_{so} W$.

**Theorem:** Let $Z \sim TLMOGom-G(z;b_1,\delta,\gamma,\Psi)$ and $W \sim TLMOGom-G(z;b_2,\delta,\gamma,\Psi)$, with the following pdfs:

$$\begin{aligned} f_1(z;b_1,\delta,\gamma,\Psi) &= \frac{2b_1\delta^2 g(z;\Psi)\left(\bar{G}(z;\Psi)\right)^{-\gamma-1} e^{2h(z;\Psi)}}{\left(1-\bar{\delta}e^{h(z;\Psi)}\right)^3} \\ &\times \left[1-\frac{\delta^2 e^{2h(z;\Psi)}}{\left(1-\bar{\delta}e^{h(z;\Psi)}\right)^2}\right]^{b_1-1} \end{aligned}$$

and

$$\begin{aligned} f_2(z;b_2,\delta,\gamma,\Psi) &= \frac{2b_2\delta^2 g(z;\Psi)\left(\bar{G}(z;\Psi)\right)^{-\gamma-1} e^{2h(z;\Psi)]}}{\left(1-\bar{\delta}e^{h(z;\Psi)}\right)^3} \\ &\times \left[1-\frac{\delta^2 e^{2h(z;\Psi)}}{\left(1-\bar{\delta}e^{h(z;\Psi)}\right)^2}\right]^{b_2-1}. \end{aligned}$$

If $b_1 \leq b_2$, then $\frac{f_{TLMOGom-G}(z;b_1,\delta,\gamma,\Psi)}{f_{TLMOGom-G}(z;b_2,\delta,\gamma,\Psi)}$ is decreasing in z.

**Proof:** Now considering the above pdfs, the ratio

$$\frac{f_1(z;b_1,\delta,\gamma,\Psi)}{f_2(z;b_2,\delta,\gamma,\Psi)} = \frac{f_1(z)}{f_2(z)} = \frac{b_1}{b_2}\left[1-\frac{\delta^2 e^{2h(z;\Psi)}}{\left(1-\bar{\delta}e^{h(z;\Psi)}\right)^2}\right]^{b_1-b_2}. \quad (13)$$

Differentiating equation (2.9) with respect to z, the resulting expression is as follows:

$$\begin{aligned} \frac{d}{dz}\left(\frac{f_1(z)}{f_2(z)}\right) &= \frac{2\delta^2 b_1}{b_2}(b_1-b_2)\left[1-\frac{\delta^2 e^{2h(z;\Psi)}}{\left(1-\bar{\delta}e^{h(z;\Psi)}\right)^2}\right]^{b_1-b_2-1} \\ &\times \frac{e^{2h(z;\Psi)}}{\left(1-\bar{\delta}e^{h(z;\Psi)}\right)^3} g(z;\Psi)\left(\bar{G}(z;\Psi)\right)^{-\gamma-1}. \end{aligned}$$

Hence, if $b_2 \geq b_1$, then $\frac{d}{dz}\left(\frac{f_1(z)}{f_2(z)}\right)$ will be negative. Consequently. we conclude that $Z <_{lro} W$, which implies $Z <_{hro} W$, and $Z <_{so} W$, indicating that $Z$ and $W$ are stochastically ordered.

### *2.7. Moments and Moment Generating Function*

We present the $r^{th}$ moment and moment generating function (mgf) of the $TLMOGom-G$ FoD. Suppose $Y \sim Expon-G(n+1)$ and $Z \sim TLMOGom-G(b,\delta,\gamma,\Psi)$, then from equation (2.4), the $r^{th}$ moment of the $TLMOGom-G$ FoD is

$$\mu_r' = E(Z^r) = \int_0^\infty z^r f_{TLMOGom-G}(z;b,\delta,\gamma,\Psi)dz = \sum_{n=0}^{\infty} \Upsilon_{n+1} E(Y^r),$$

with $E(Y^r)$ being the $r^{th}$ moment of the Expon-G distribution with power parameter (n+1), and $\Upsilon_{n+1}$ as in equation (2.5).

The Moment generating function (mgf) is

$$M_t(Z) = E(e^{tZ}) = \sum_{r=0}^{\infty} \frac{t^r}{r!} E(Z^r) = \sum_{n=0}^{\infty} \Upsilon_{n+1} M_Y(t),$$

where $M_Y(t)$ is the mgf of the Expon-G distribution.

## 3. Special cases

Three special cases were considered where the baseline distributions are Pareto (P), Weibull (W) and log-logistic (LLo), respectively.

### *3.1. Topp-Leone-Marshall-Olkin-Gompertz-Pareto (TLMOGom-P) Distribution*

Suppose the Pareto distribution is the baseline distribution with pdf and cdf $g(z;\omega) = \omega(1+z)^{-(\omega+1)}$ and $G(z;\omega) = 1-(1+z)^{-\omega}$, for $\omega > 0$, then the cdf, pdf and hrf of the TLMOGom-P distribution are

$$F_{TLMOGom-P}(z;\delta,b,\gamma,\omega) = \left[1 - \frac{\delta^2 e^{\frac{2}{\gamma}(h(z;\gamma,\omega))}}{\left(1-\bar{\delta}e^{\frac{1}{\gamma}(h(z;\gamma,\omega))}\right)^2}\right]^b,$$

$$\begin{aligned} f_{TLMOGom-P}(z;\delta,b,\gamma,\omega) &= \frac{2b\delta^2\omega\,(1+z)^{\omega\gamma+1}\,e^{\frac{2}{\gamma}(h(z;\gamma,\omega))}}{\left(1-\bar{\delta}e^{\frac{1}{\gamma}(h(z;\gamma,\omega))}\right)^3} \\ &\times \left[1 - \frac{\delta^2 e^{\frac{2}{\gamma}(h(z;\gamma,\omega))}}{\left(1-\bar{\delta}e^{\frac{1}{\gamma}(h(z;\gamma,\omega))}\right)^2}\right]^{b-1} \end{aligned}$$

and

$$
\begin{aligned}
h_{TLMOGom-P}(z;\delta,b,\gamma,\omega) &= \frac{2b\delta^2\omega\,(1+z)^{\omega\gamma+1}\,e^{\frac{2}{\gamma}(h(z;\gamma,\omega))}}{\left(1-\bar{\delta}e^{\frac{1}{\gamma}(h(z;\gamma,\omega))}\right)^3} \\
&\times \left[1-\frac{\delta^2 e^{\frac{2}{\gamma}(h(z;\gamma,\omega))}}{\left(1-\bar{\delta}e^{\frac{1}{\gamma}h(z;\gamma,\omega)}\right)^2}\right]^{b-1} \\
&\times \left\{1-\left[1-\frac{\delta^2 e^{\frac{2}{\gamma}(h(z;\gamma,\omega))}}{\left(1-\bar{\delta}e^{\frac{1}{\gamma}(h(z;\gamma,\omega))}\right)^2}\right]^{b}\right\}^{-1},
\end{aligned}
$$

respectively, for $\delta, b, \gamma, \omega > 0$, where $h(z;\gamma,\omega) = 1-[1+z]^{\omega\gamma}$ and $\bar{\delta} = 1-\delta$.

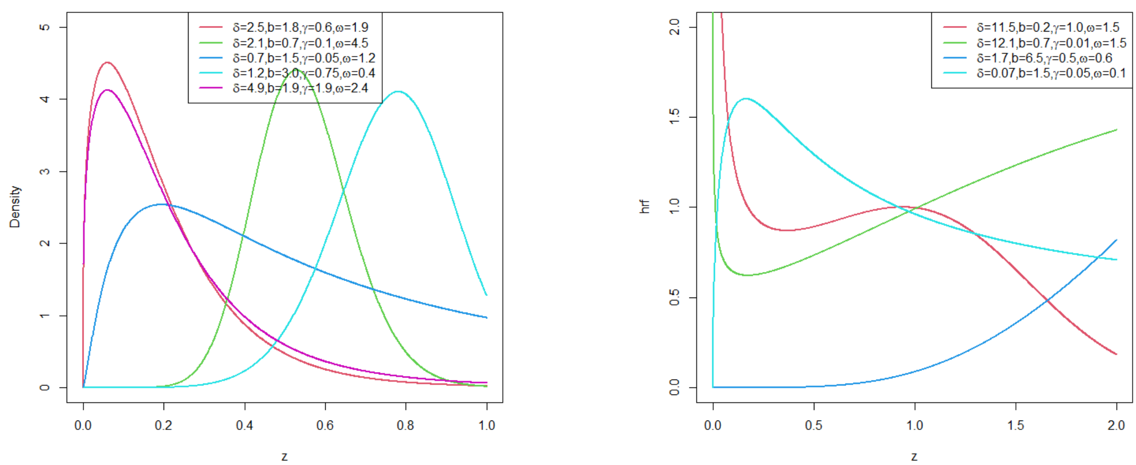


Figure 1. TLMOGom-P pdf and hrf plots

We can deduce from Figure [1] that this new distribution handles almost symmetric, skewed to the left and skewed to the right data. The distribution can fit data sets with hrf that are bathtub followed by upside bathtub, bathtub and increasing shapes.

Figure [2] illustrates the spread and peakedness behaviours of the TLMOGom-P as follows:

- When the values of $b$ and $\omega$ are set, kurtosis and skewness vary as we adjust $\gamma$ and $\delta$.
- When we fix the values of $\delta$ and $\gamma$, kurtosis and skewness increase as $b$ and $\omega$ increase.

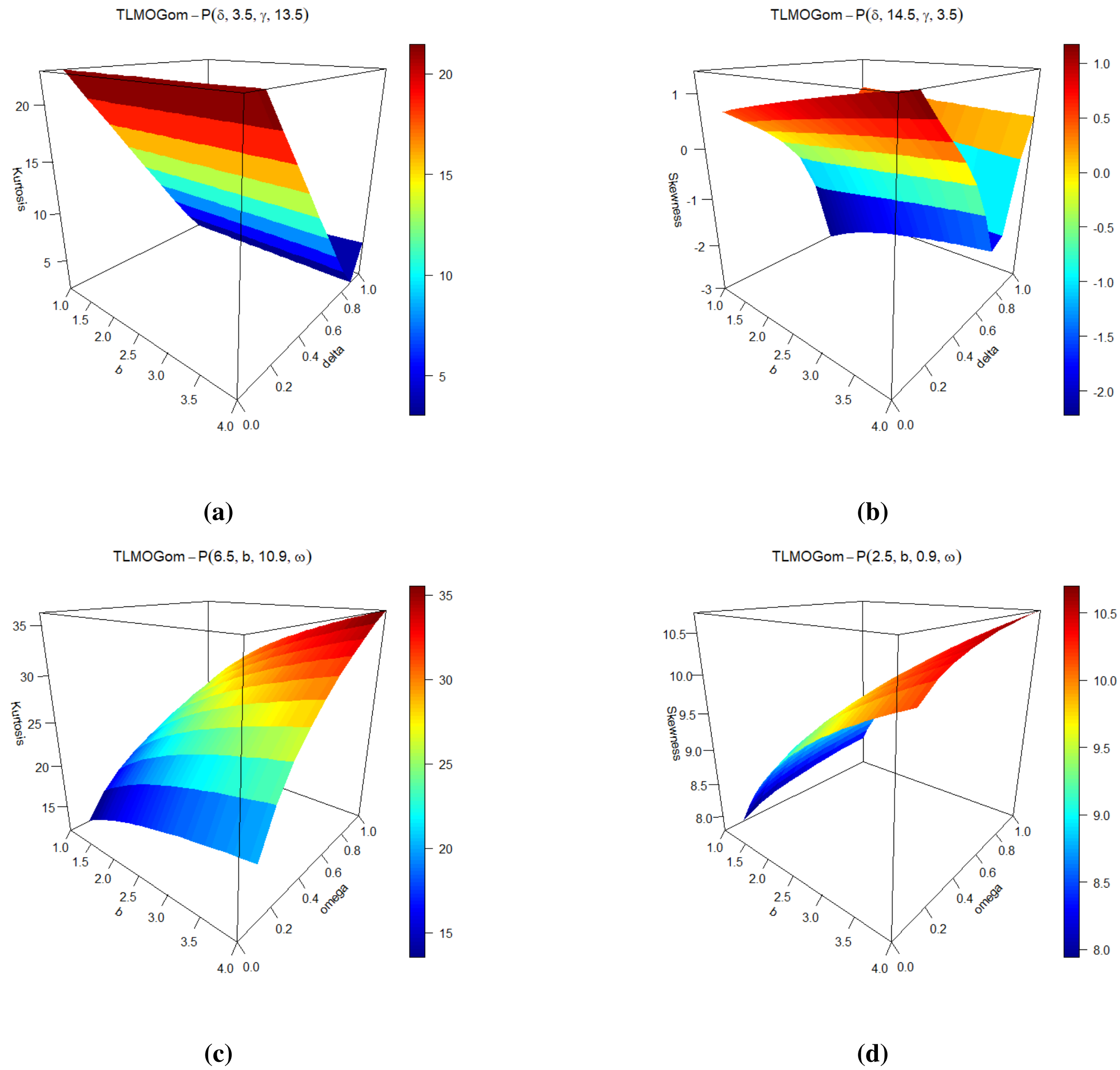


Figure 2. TLMOGom-P kurtosis and skewness plots

### 3.2. *Topp-Leone-Marshall-Olkin-Gompertz-Weibull (TLMOGom-W) Distribution*

Consider the Weibull distribution with cdf and pdf $G(z;\lambda) = 1 - e^{-z^{\lambda}}$ and $g(z;\lambda) = \lambda z^{\lambda-1} e^{-z^{\lambda}}$, for $\lambda > 0$, repectively. The cdf, pdf and hrf of the TLMOGom-W distribution are:

$$F_{TLMOGom-W}(z;\delta,b,\gamma,\lambda) = \left[1 - \frac{\delta^2 e^{\frac{2}{\gamma}(h(z;\gamma,\lambda))}}{\left(1 - \bar{\delta} e^{\frac{1}{\gamma}(h(z;\gamma,\lambda))}\right)^2}\right]^b,$$

$$
\begin{aligned}
f_{TLMOGom-W}(z;\delta,b,\gamma,\lambda) &= \frac{2b\delta^2\lambda z^{\lambda-1}e^{\gamma z^\lambda}e^{\frac{2}{\gamma}(h(z;\gamma,\lambda))}}{\left(1-\bar{\delta}e^{\frac{1}{\gamma}(h(z;\gamma,\lambda))}\right)^3} \\
&\times \left[1-\frac{\delta^2 e^{\frac{2}{\gamma}(h(z;\gamma,\lambda))}}{\left(1-\bar{\delta}e^{\frac{1}{\gamma}(h(z;\gamma,\lambda))}\right)^2}\right]^{b-1},
\end{aligned}
$$

and

$$
\begin{aligned}
h_{TLMOGom-W}(z;\delta,b,\gamma,\lambda) &= \frac{2b\delta^2\lambda z^{\lambda-1}e^{\gamma z^\lambda}e^{\frac{2}{\gamma}(h(z;\gamma,\lambda))}}{\left(1-\bar{\delta}e^{\frac{1}{\gamma}(h(z;\gamma,\lambda))}\right)^3} \\
&\times \left[1-\frac{\delta^2 e^{\frac{2}{\gamma}(h(z;\gamma,\lambda))}}{\left(1-\bar{\delta}e^{\frac{1}{\gamma}(h(z;\gamma,\lambda))}\right)^2}\right]^{b-1} \\
&\times \left\{1-\left[1-\frac{\delta^2 e^{\frac{2}{\gamma}(h(z;\gamma,\lambda))}}{\left(1-\bar{\delta}e^{\frac{1}{\gamma}(h(z;\gamma,\lambda))}\right)^2}\right]^{b}\right\}^{-1},
\end{aligned}
$$

respectively, for $\delta, b, \lambda, \gamma > 0$, where $h(z;\gamma,\lambda) = 1 - e^{\gamma z^\lambda}$, and $\bar{\delta} = 1 - \delta$.

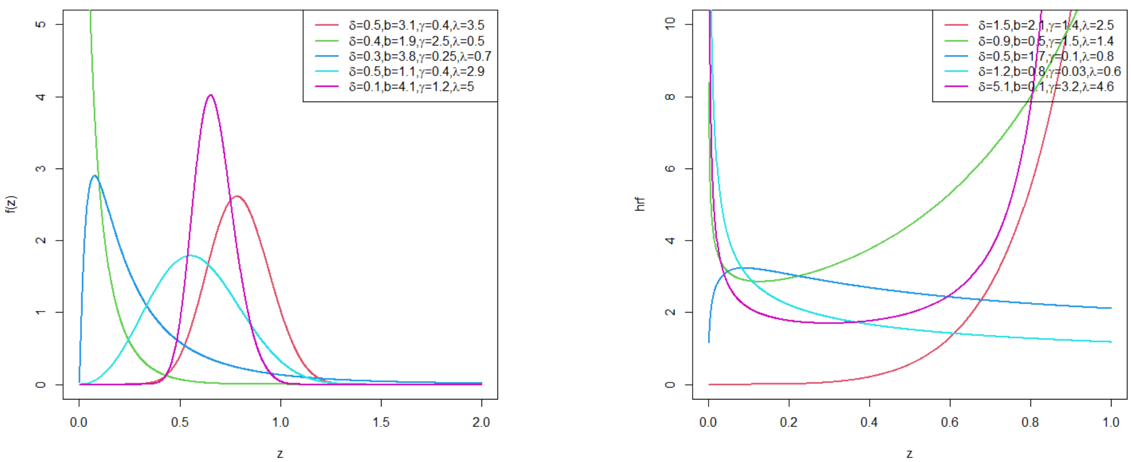


Figure 3. TLMOGom-W pdf and hrf plots

This model can handle almost symmetric data, peaked, reverse-J, skewed to the right and reverse-J. The hrf can take bathtub, upside down bathtub, decreasing and increasing shapes.
Figure [4] illustrates the spread and peakedness behaviors of the TLMOGomW as follows:

- When we fix the values of $\lambda$ and $b$, kurtosis decreases as $\delta$ increases and increases as $\gamma$ increases. Skewness decreases as $\gamma$ and $\delta$ increase.
- When we fix the values of $\delta$ and $\lambda$, kurtosis increases as $b$ increases and skewness decreases as $\gamma$ increases.

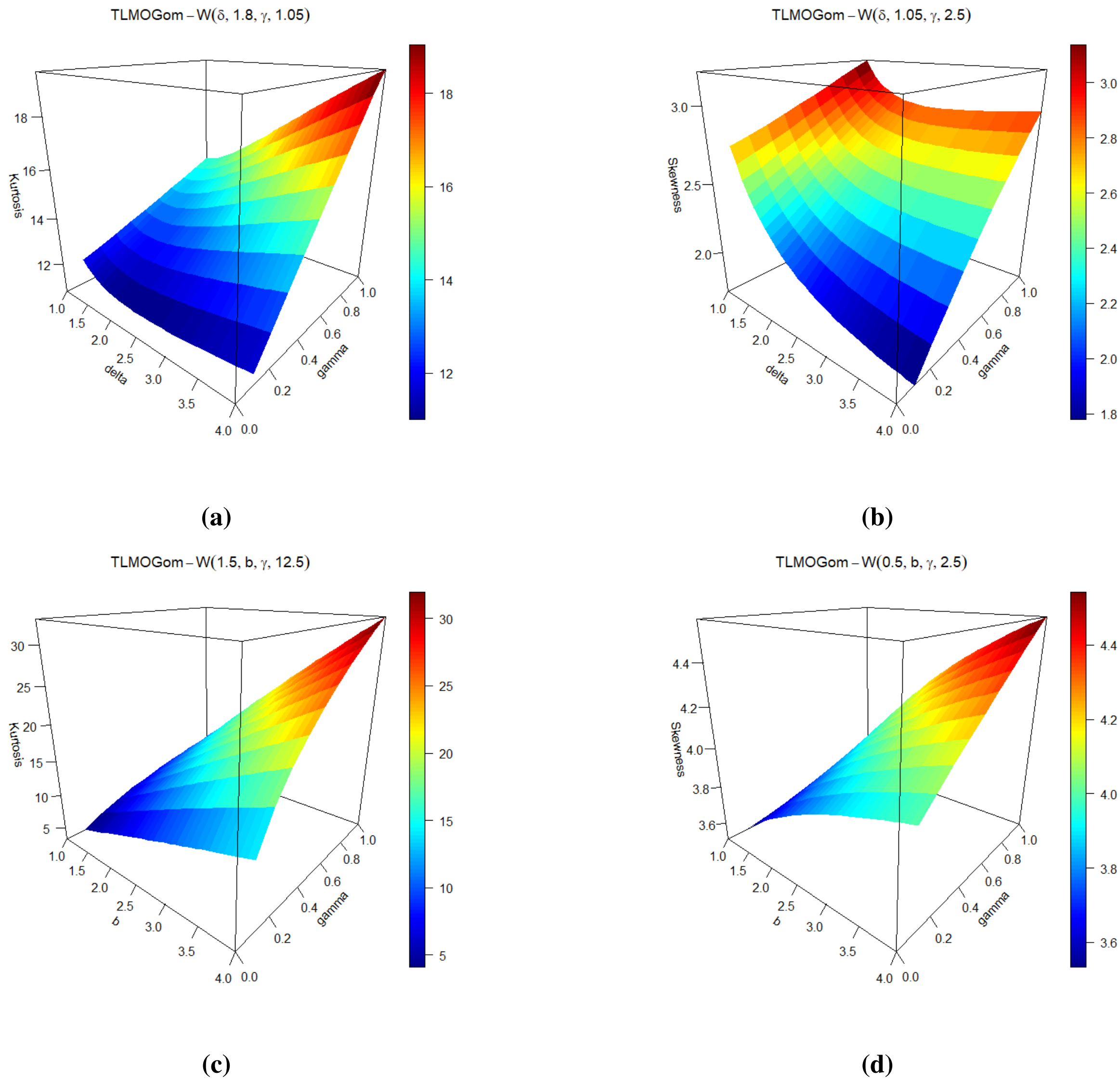


Figure 4. TLMOGom-W kurtosis and skewness plots

### *3.3. Topp-Leone-Marshall-Olkin-Gompertz-Log-logistic (TLMOGom-LLo) Distribution*

Consider the log-logistic distribution with the pdf $g(z;c) = cz^{c-1}(1+z^c)^{-2}$ and cdf $G(z;c) = 1-(1+z^c)^{-1}$, for $c > 0$. Let $h(z;\gamma,c) = \frac{1}{\gamma}\left[1-(1+z^c)^{\gamma}\right]$. The cdf, pdf and hrf of the TLMOGom-LLo distribution are:

$$F_{TLMOGom-LLo}(z;\delta,b,\gamma,c) = \left[1 - \frac{\delta^2 e^{2h(z;\gamma,c)}}{\left(1-\bar{\delta}e^{h(z;\gamma,c)}\right)^2}\right]^b,$$

$$
\begin{aligned}
f_{TLMOGom-LLo}(z;\delta,b,\gamma,c) &= \frac{2b\delta^2 cz^{-1}\left(1+z^c\right)^{\gamma-1}e^{2h(z;\gamma,c)}}{\left(1-\bar{\delta}e^{h(z;\gamma,c)}\right)^3} \\
&\times \left[1-\frac{\delta^2 e^{2h(z;\gamma,c)}}{\left(1-\bar{\delta}e^{h(z;\gamma,c)}\right)^2}\right]^{b-1}
\end{aligned}
$$

and

$$
\begin{aligned}
h_{TLMOGom-LLo}(z;\delta,b,\gamma,c) &= \frac{2b\delta^2 cz^{-1}\left(1+z^c\right)^{\gamma-1}e^{2h(z;\gamma,c)}}{\left(1-\bar{\delta}e^{h(z;\gamma,c)}\right)^3} \\
&\times \left[1-\frac{\delta^2 e^{2h(z;\gamma,c)}}{\left(1-\bar{\delta}e^{h(z;\gamma,c)}\right)^2}\right]^{b-1} \\
&\times \left\{1-\left[1-\frac{\delta^2 e^{2h(z;\gamma,c)}}{\left(1-\bar{\delta}e^{h(z;\gamma,c)}\right)^2}\right]^{b}\right\}^{-1},
\end{aligned}
$$

for $\delta, b, \gamma, c > 0$, and $\bar{\delta} = 1-\delta$.

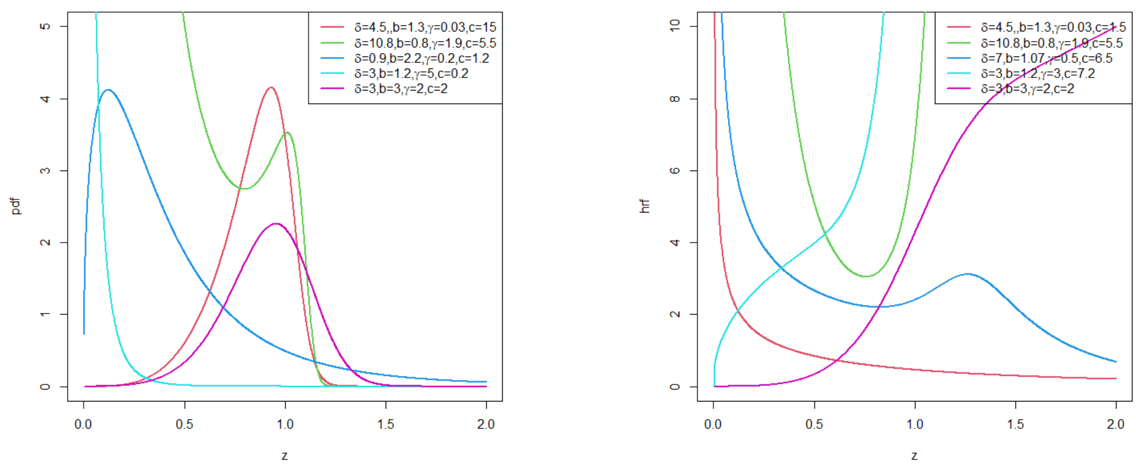


Figure 5. TLMOGom-LLo pdf and hrf plots

Fig [3.5] shows that the model works well with data that are left and right-skewed, and reverse-J. It fits to many hrfs that include the uni-modal, increasing, decreasing, bathtub followed by upside down bathtub.

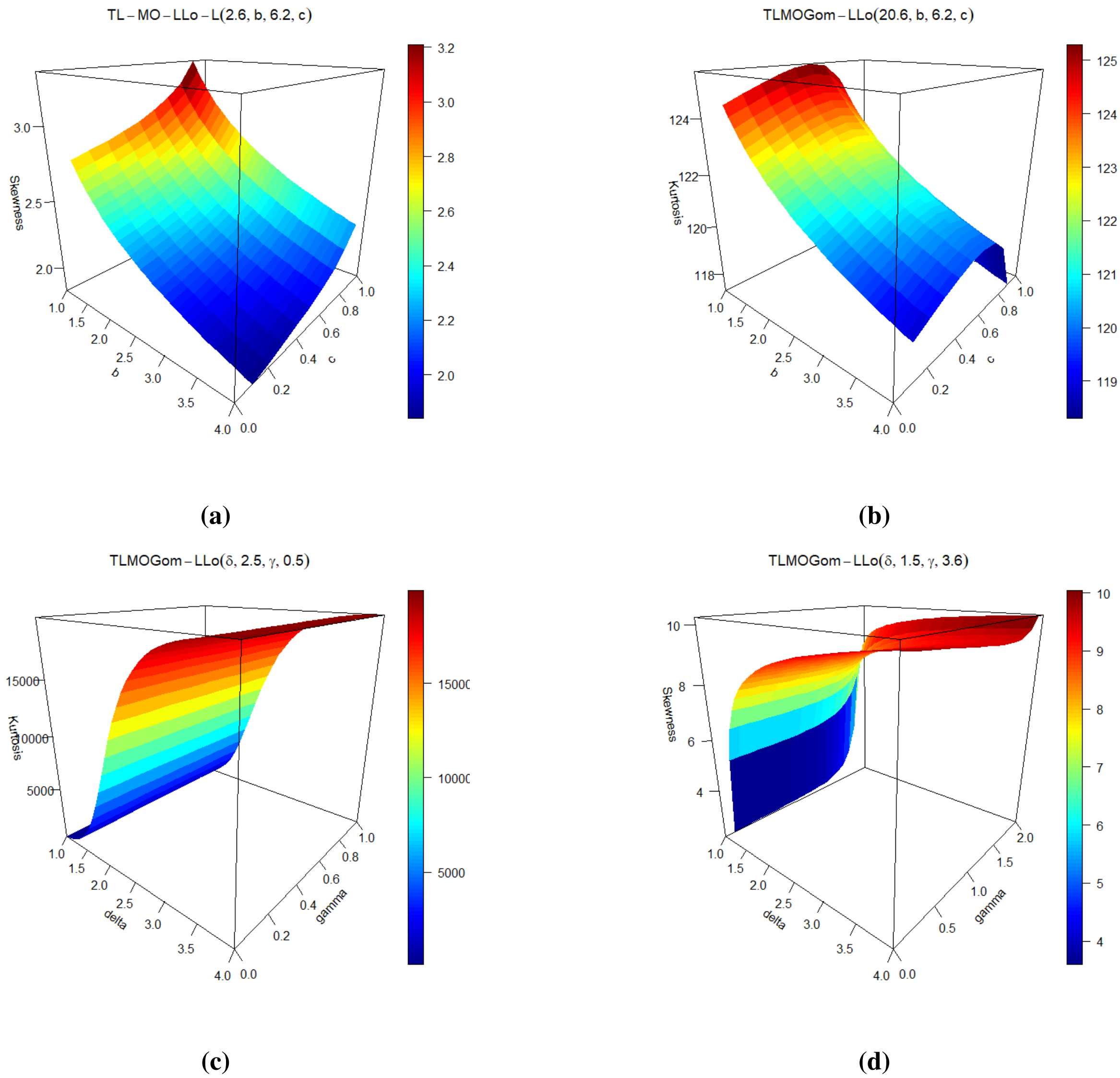


Figure 6. TLMOGom-LLo kurtosis and skewness plots

In Figure [6], the skewness and kurtosis behaviors of the TLMO-LLo are depicted as follows:

- When we fix the values of $\delta$ and $\gamma$, kurtosis and skewness levels of the TLMO-LLo decrease as both $b$ and $c$ increase.
- As the values of $\delta$ and $\gamma$ increase, various levels of kurtosis are observed for the TLMO-LLo distribution are observed when the values of $b$ and $c$ are held constant.

## 4. Estimation Methods

In this section, our primary objective is to estimate the unknown parameters of the $TLMOGom-W$ using multiple estimation techniques, including maximum likelihood estimation (MLE), least squares (LS), weighted least squares (WLS), Cramér-von Mises (CVM) and Anderson-Darling (AD). The optimization process for parameter estimation followed an iterative approach, beginning with an initial set of parameter estimates informed by domain knowledge and preliminary data analysis. To enhance robustness, multiple random initializations were tested, and the one yielding the best objective function value (negative log-likelihood for MLE, sum of squared errors for LS and WLS, Cramér-von Mises statistic for CVM or Anderson-Darling statistic for AD) was selected. During each iteration, parameter estimates were updated according to the respective estimation algorithm, and convergence was assessed by monitoring the stabilization of the objective function. The iterations continued until the objective function reached a stable value, indicating that the parameters had converged to an optimal solution. This combination of iterative refinement, informed initialization, and convergence monitoring ensures that the final parameter estimates are reliable and accurate. By incorporating multiple estimation methods, the approach provides a comprehensive and robust framework for parameter estimation, reducing sensitivity to initial parameter choices and improving the overall reliability of the fitted distribution.

Below we look at the derivation of the parameter estimates for the five different techniques. Let $\triangle = (\delta, b, \gamma, \lambda)^T$ denote the parameters vector. Also let $X_{(1)}$, $X_{(2)}$,......,$X_{(m)}$ be the ordered statistics from the $TLMOGom-W(\delta, b, \gamma, \lambda)$ distribution with sample size m and $x_{(1)}$, $x_{(2)}$,.....,$x_{(m)}$ be the ordered observed values.

### 4.1. MLE Approach

This method is one of the most used techniques for parameter estimation. In practice, the MLEs are often reliable, and large sample theory provides convenient estimates to the parameters that yield good results even with limited data. Now, if $Z_i \sim TLMOGom-W(\delta, b, \gamma, \lambda)$, then the log-likelihood function $l = l(\triangle)$, based on a random sample of size m, is

$$\begin{aligned} l &= mln(2) + mln(b) + mln(\lambda) + 2ln(\delta) + (\lambda-1)\sum_{i=1}^{m} ln(z_i) + \gamma \sum_{i=1}^{m} z_i^{\lambda} \\ &+ \frac{2}{\gamma}\sum_{i=1}^{m}\left(1-e^{\gamma\sum_{i=1}^{m} z_i^{\lambda}}\right) - 3\sum_{i=1}^{m} ln\left(1-(1-\delta)e^{\frac{1}{\gamma}\left(1-e^{\gamma\sum_{i=1}^{m} z_i^{\lambda}}\right)}\right) \\ &+ (b-1)\sum_{i=1}^{m} ln\left(1-\frac{\delta^2 e^{\frac{2}{\gamma}\left(1-e^{\gamma\sum_{i=1}^{m} z_i^{\lambda}}\right)}}{1-(1-\delta)e^{\frac{1}{\gamma}\left(1-e^{\gamma\sum_{i=1}^{m} z_i^{\lambda}}\right)}}\right). \end{aligned}$$

Parameter estimates are obtained by solving the non-linear equations $\frac{\partial l}{\partial \delta} = 0$, $\frac{\partial l}{\partial b} = 0$, $\frac{\partial l}{\partial \gamma} = 0$ and $\frac{\partial l}{\partial \lambda} = 0$. See Appendix for the derivation of the partial derivatives.

### 4.2. LS Approach

According to Swain et al. [38], unknown parameters are determined via minimization of the function:

$$\begin{aligned} LS(\triangle) &= \sum_{i=1}^{m}\left(F_{TLMOGom-W}(z_{(i)};\delta,b,\gamma,\lambda) - \frac{1}{m+1}\right)^2 \\ &= \sum_{i=1}^{m}\left\{\left[1-\frac{\delta^2 e^{2h(z_{(i)};\gamma,\lambda)}}{\left(1-\bar{\delta}e^{h(z_{(i)};\gamma,\lambda)}\right)^2}\right]^b - \frac{1}{m+1}\right\}^2. \end{aligned}$$

Parameter estimates are obtained by taking partial derivatives with respect to the parameters and equate to zero. The resulting non-linear equations are numerically solved to get the parameter estimates.

### 4.3. WLS Approach

The parameter estimates for the WLS approach are obtained through minimization of the following function:

$$
\begin{aligned}
WLS(\triangle) &= \sum_{i=1}^{m} \frac{(1+m)^2(2+m)}{(m-i+1)i} \left( F_{TLMOGom-W}(z_{(i)}; \delta, b, \gamma, \lambda) - \frac{i}{1+m} \right)^2 \\
&= \sum_{i=1}^{m} \frac{(1+m)^2(2+m)}{(m-i+1)i} \left( \left[ 1 - \frac{\delta^2 e^{2h(z_{(i)};\gamma,\lambda)}}{\left(1-\bar{\delta} e^{h(z_{(i)};\gamma,\lambda)}\right)^2} \right]^b - \frac{i}{1+m} \right)^2 .
\end{aligned}
$$

### *4.4. CVM Approach*

The parameter estimates are found by minimising $C(\triangle)$ with respect to the unknown parameters in the CVM function

$$
\begin{aligned}
C(\triangle) &= \frac{1}{12} + \sum_{i=1}^{m} \left( F_{TLMOGom-W}(z_{(i)}; \delta, b, \gamma, \lambda) - \frac{2i-1}{2m} \right)^2 \\
&= \frac{1}{12} + \sum_{i=1}^{m} \left( \left[ 1 - \frac{\delta^2 e^{2h(z_{(i)};\gamma,\lambda)}}{\left(1-\bar{\delta} e^{h(z_{(i)};\gamma,\lambda)}\right)^2} \right]^b - \frac{2i-1}{2m} \right)^2 .
\end{aligned}
$$

### *4.5. AD Approach*

The AD test is employed to assess whether a given sample of data is derived from a population that follows a specific distribution. Deducing from a paper by Lewis [26], the function containing the model parameters is given by

$$
\begin{aligned}
AD(\triangle) &= -m - \frac{1}{m} \sum_{i=1}^{m} (2i-1) \ln \left[ F(z_{(i)}; \delta, b, \gamma, \lambda) \right] + \ln \left[ S(z_{(m+1-i)}; \delta, b, \gamma, \lambda) \right] \\
&= -m - \frac{1}{m} \sum_{i=1}^{m} (2i-1) \ln \left[ \left( 1 - \frac{\delta^2 e^{2h(z_{(i)};\gamma,\lambda)}}{\left(1-\bar{\delta} e^{h(z_{(i)};\gamma,\lambda)}\right)^2} \right)^b \right] \\
&- \frac{1}{m} \sum_{i=1}^{m} (2i-1) \ln \left[ 1 - \left( 1 - \frac{\delta^2 e^{2h(z_{(i)};\gamma,\lambda)}}{\left(1-\bar{\delta} e^{h(z_{(i)};\gamma,\lambda)}\right)^2} \right)^b \right],
\end{aligned}
$$

and the estimates emanate from minimising the function with respect to the parameters.

## 5. Simulations

In this section, we examine the performance of the TLMOGom-W distribution through a simulation study conducted to make comparisons of the different estimation methods for varying sample sizes (m = 25, 50, 100, 200, 400, and 800) using the R software program. To achieve this, we shall employ:

- Average Bias (Abias) which is the average of the biases calculated across multiple estimation samples. It provides an overall measure of the tendency of the estimation method to consistently overestimate or underestimate the true parameter.
- Root Mean Square Error (RMSE), which is a measure of the average magnitude of the errors between predicted values and observed values. It combines both bias and variability in the predictions.

It should be noted that there are several computational issues in R which include:

- Slowness with operations on large datasets especially with complex calculations or iterative simulations. Use of the packages like $ff$ or $bigmemory$ is recommended.
- Convergence issues may arise when fitting complex models. Apart from adjusting starting values and increasing the number of iterations it is also advisable to choose different optimization algorithms such as $aptim$ and $nlminb$.
- Results obtained from complex models may be difficult to interpret or communicate effectively. Utilizing visualization tools such as $ggplot2$ may help with communicating the results.
- Some algorithms may be computationally intensive, resulting in long run times. Code profiling using $profvis$ package may cut down the run times via bottlenecks identification and optimization of the slowest parts.

Tables [1] and [2] provide values of the parameter estimates, as well as the associated rank in relation to the predetermined value, for each estimation method as we vary the sample sizes.

Table 1. **Simulation results for** $\delta = 0.01, b = 0.8, \gamma = 0.6, \lambda = 1.04$

| | | RMSE | | | | | Abias | | | | |
|---|---|---|---|---|---|---|---|---|---|---|---|
| $m$ | Parameter | MLE | WLS | LS | CVM | AD | MLE | WLS | LS | CVM | AD |
| 25 | $\delta$ | 0.0308 (1) | 6.0032 (2) | 6.1656 (3) | 6.1719 (4) | 6.2466 (5) | 0.0075 (1) | 0.9348 (2) | 0.9682 (3) | 0.9702 (4) | 0.9872 (5) |
| | $b$ | 15.7956 (5) | 4.0280 (1) | 4.1226 (2) | 4.1302 (3) | 4.1870 (4) | 3.7842 (5) | -0.6177 (1) | -0.6420 (2) | -0.6443 (4) | -0.6423 (3) |
| | $\gamma$ | 0.5763 (1) | 2.7893 (2) | 3.0749 (4) | 3.0404 (3) | 3.7782 (5) | 0.1371 (3) | 0.1614 (4) | -0.0278 (2) | -0.0101 (1) | -0.5970 (5) |
| | $\lambda$ | 0.2981 (1) | 0.8394 (4) | 0.6972 (3) | 0.6488 (2) | 1.0428 (5) | -0.0929 (5) | -0.0632 (3) | -0.0550 (2) | -0.0527 (1) | -0.0686 (4) |
| | $\sum$ranks | 8 | 9 | 12 | 12 | 19 | 14 | 10 | 9 | 10 | 17 |
| 50 | $\delta$ | 0.0230 (1) | 4.2645 (2) | 4.4207 (5) | 4.4144 (4) | 4.3878 (3) | 0.0052 (1) | 0.9403 (2) | 0.9882 (5) | 0.9861 (4) | 0.9792 (3) |
| | $b$ | 7.9445 (5) | 2.8690 (1) | 2.9419 (2) | 2.9447 (3) | 2.9571 (4) | 1.3918 (5) | -0.6265 (1) | -0.6548 (3) | -0.6561 (4) | -0.6454 (2) |
| | $\gamma$ | 0.4427 (1) | 2.0070 (2) | 2.2096 (3) | 2.2207 (4) | 2.6696 (5) | 0.0724 (2) | 0.1632 (4) | -0.0537 (1) | -0.0766 (3) | -0.5964 (5) |
| | $\lambda$ | 0.2318 (1) | 0.5635 (4) | 0.3435(3) | 0.3057 (2) | 0.6659 (5) | -0.0724 (5) | -0.0605 (3) | -0.0454 (2) | -0.0442 (1) | -0.0629 (4) |
| | $\sum$ranks | 8 | 9 | 13 | 13 | 17 | 13 | 10 | 11 | 12 | 14 |
| 100 | $\delta$ | 0.0104 (1) | 3.0660 (3) | 3.1305 (5) | 3.1294 (4) | 3.0548 (2) | 0.0025 (1) | 0.9615 (3) | 0.9899 (5) | 0.9895 (4) | 0.9614 (2) |
| | $b$ | 2.8459 (5) | 2.0390 (1) | 2.0880 (2) | 2.0855 (3) | 2.0871 (4) | 0.4879 (1) | -0.6312 (2) | -0.6586 (5) | -0.6561 (4) | -0.6498 (3) |
| | $\gamma$ | 0.2788 (1) | 1.4359 (2) | 1.7050 (3) | 1.7333 (4) | 1.8830 (5) | 0.0291 (1) | 0.1314 (2) | -0.2862 (3) | -0.3269 (4) | -0.5952 (5) |
| | $\lambda$ | 0.1690 (1) | 0.4108 (5) | 0.1976 (2) | 0.2471(3) | 0.3860 (4) | -0.0553 (4) | -0.0593 (5) | -0.0425 (1) | -0.0451 (2) | -0.0550(3) |
| | $\sum$ranks | 8 | 11 | 12 | 14 | 15 | 7 | 12 | 14 | 14 | 13 |
| 200 | $\delta$ | 0.0153 (1) | 2.1924 (3) | 2.2128 (5) | 2.2112 (4) | 2.0870(2) | 0.0023 (1) | 0.9767 (3) | 0.9894 (5) | 0.9886 (4) | 0.9227 (2) |
| | $b$ | 2.6620 (5) | 1.4512 (1) | 1.4736 (3) | 1.4699 (2) | 1.4742 (4) | 0.4791 (1) | -0.6419 (2) | -0.6528 (4) | -0.6484 (3) | -0.6565 (5) |
| | $\gamma$ | 0.2400 (1) | 1.0225 (2) | 1.3292 (4) | 1.3275 (3) | 1.3310 (5) | 0.0234 (1) | 0.1177 (2) | -0.5811 (4) | -0.5780 (3) | -0.5942 (5) |
| | $\lambda$ | 0.1497 (1) | 0.2300 (4) | 0.2210 (3) | 0.2598 (5) | 0.1630 (2) | -0.0413 (1) | -0.0512 (4) | -0.0490 (3) | -0.0532 (5) | -0.0442 (2) |
| | $\sum$ranks | 8 | 10 | 15 | 14 | 13 | 4 | 11 | 16 | 15 | 14 |
| 400 | $\delta$ | 0.0033 (1) | 1.5566 (3) | 1.5743 (4) | 1.8537 (5) | 1.4560 (2) | $4.6562\times10^{-4}$ (1) | 0.9828 (3) | 0.9893 (5) | 0.9890 (4) | 0.9073 (2) |
| | $b$ | 0.2345 (1) | 1.0294 (3) | 1.0083 (2) | 1.4743 (5) | 1.0434 (4) | 0.1306 (1) | -0.6464 (3) | -0.6430 (2) | -0.6586 (4) | -0.6599 (5) |
| | $\gamma$ | 0.0139 (1) | 0.7223 (2) | 0.9230 (4) | 0.8971 (3) | 0.9422 (5) | -0.0041 (1) | 0.1234 (2) | -0.1365 (4) | -0.1266 (3) | -0.5956 (5) |
| | $\lambda$ | 0.0890 (3) | 0.1346 (5) | 0.0878 (2) | 0.0896 (4) | 0.0654 (1) | -0.0246 (1) | -0.0469 (5) | -0.0439 (3) | -0.0443 (4) | -0.0405 (2) |
| | $\sum$ranks | 6 | 13 | 12 | 17 | 12 | 4 | 13 | 14 | 15 | 14 |
| 800 | $\delta$ | $3.1903\times10^{-5}$ (1) | 1.1040 (5) | 0.9990 (3) | 1.0367 (4) | 1.0098 (2) | $-3.1903\times10^{-5}$ (1) | 0.9863 (4) | 0.8900 (3) | 0.9945 (5) | 0.8869 (2) |
| | $b$ | 0.0195 (1) | 0.7293 (2) | 0.7335 (4) | 0.0.8010 (5) | 0.7370 (3) | 0.0195 (1) | -0.6503 (2) | -0.6511 (3) | -0.6672 (5) | -0.6592 (4) |
| | $\gamma$ | $7.3051\times10^{-5}$ (1) | 0.5073 (2) | 0.5082 (3) | 0.5962 (4) | 0.6658 (5) | $7.3051\times10^{-5}$ (1) | 0.1389 (2) | -0.1400 (3) | -0.1574 (4) | -0.5952 (5) |
| | $\lambda$ | 0.0115 (1) | 0.0720 (3) | 0.0737 (4) | 0.0804 (4) | 0.0450 (2) | 0.0115 (1) | -0.0430 (3) | -0.0556 (4) | -0.0571 (5) | -0.0402 (2) |
| | $\sum$ranks | 4 | 12 | 14 | 17 | 12 | 4 | 11 | 13 | 19 | 13 |

Table [5.1] shows that the average bias (Abias) decreases with increasing sample size. Additionally, the RMSE decreased as the sample size increased for all estimation methods. The stability of the TLMOGom-W distribution is evident from the results as indicated by the modest ABIAS and RMSE values for all four model parameters.
Based on the results in Table [5.2], the MLE and WLS methods yielded comparable results in estimating the TLMOGom-W parameters. The MLE method achieved the best performance, followed by WLS, with the LS method coming next. Conversely, the CVM method demonstrated the least favourable performance among the estimation methods.

Table 2. **Rankings of Estimation Techniques for the TLMOGom-W Distribution: Partial and Overall Ranks**

| Parameters | $m$ | MLE | WLS | LS | CVM | AD |
|---|---|---|---|---|---|---|
| $\delta = 0.01, b = 0.8, \gamma = 0.6, \lambda = 1.04$ | 25 | 22 $^{(3.5)}$ | 19 $^{(1)}$ | 21 $^{(2)}$ | 22 $^{(3.5)}$ | 36 $^{(5)}$ |
| | 50 | 21 $^{(2)}$ | 19 $^{(1)}$ | 24 $^{(3)}$ | 27 $^{(4)}$ | 31 $^{(5)}$ |
| | 100 | 15 $^{(1)}$ | 23 $^{(2)}$ | 26 $^{(3)}$ | 28 $^{(4.5)}$ | 28 $^{(4.5)}$ |
| | 200 | 12 $^{(1)}$ | 21 $^{(2)}$ | 27 $^{(3)}$ | 31 $^{(5)}$ | 28 $^{(4)}$ |
| | 400 | 10 $^{(1)}$ | 26 $^{(3.5)}$ | 26 $^{(3.5)}$ | 32 $^{(5)}$ | 25 $^{(2)}$ |
| | 800 | 8 $^{(1)}$ | 23 $^{(3)}$ | 27 $^{(4)}$ | 36 $^{(5)}$ | 15 $^{(2)}$ |
| $\sum$ranks | | 9.5 | 12.5 | 18.5 | 27 | 22.5 |
| Overall rank | | 1 | 2 | 3 | 5 | 4 |

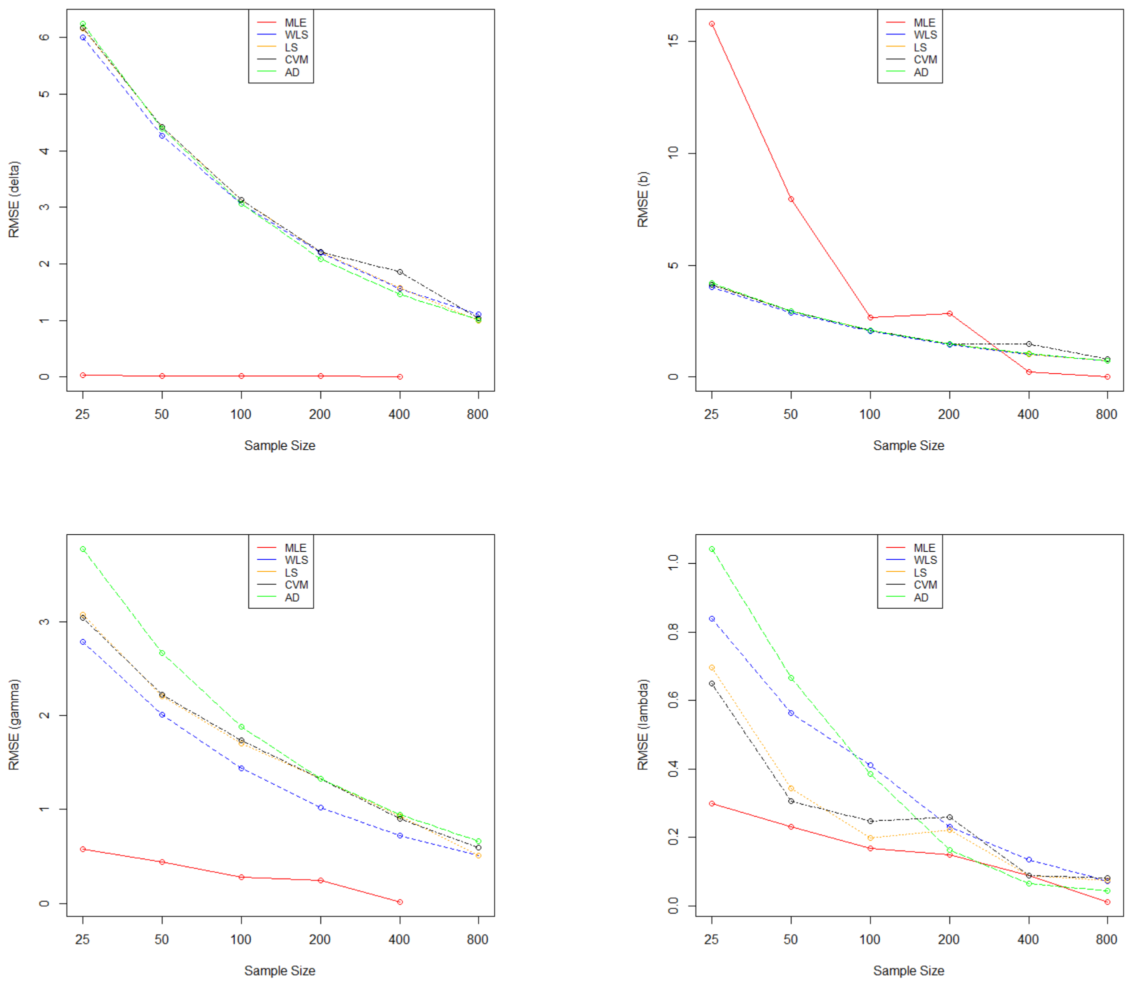


Figure 7. TLMOGom-W RMSE Plots

Table 3. **Simulation results for $\delta = 0.7, b = 0.7, \gamma = 0.9, \lambda = 0.9$**

| | | | | RMSE | | | | | Abias | | |
|---|---|---|---|---|---|---|---|---|---|---|---|
| $m$ | Parameter | MLE | WLS | LS | CVM | AD | MLE | WLS | LS | CVM | AD |
| | $\delta$ | 1.4247 $^{(1)}$ | 1.8800 $^{(2)}$ | 1.8965 $^{(3.5)}$ | 1.8965 $^{(3.5)}$ | 1.8974 $^{(5)}$ | 0.1396 $^{(1)}$ | 0.2893 $^{(2)}$ | 0.2998 $^{(3.5)}$ | 0.2998 $^{(3.5)}$ | 0.2999 $^{(5)}$ |
| 25 | $b$ | 2.0122 $^{(5)}$ | 1.3315 $^{(1)}$ | 1.8870 $^{(2)}$ | 1.8871 $^{(3)}$ | 1.8974 $^{(4)}$ | 2.2432 $^{(5)}$ | 0.0020 $^{(1)}$ | 0.2751 $^{(3)}$ | 0.2747 $^{(2)}$ | 0.2973 $^{(4)}$ |
| | $\gamma$ | 3.4705 $^{(1)}$ | 3.6213 $^{(2)}$ | 5.6053 $^{(3)}$ | 5.6066 $^{(4)}$ | 5.6276 $^{(5)}$ | 0.8746 $^{(2)}$ | -0.4260 $^{(1)}$ | -0.8782 $^{(3)}$ | -0.8784 $^{(4)}$ | -0.8897 $^{(5)}$ |
| | $\lambda$ | 0.8780 $^{(1)}$ | 1.4495 $^{(2)}$ | 3.3798 $^{(3)}$ | 3.3964 $^{(4)}$ | 3.4918 $^{(5)}$ | 0.2260 $^{(2)}$ | -0.0037 $^{(1)}$ | -0.5093 $^{(3)}$ | -0.5117 $^{(4)}$ | -0.5483 $^{(5)}$ |
| | $\sum$ranks | 8 | 7 | 11.5 | 14.5 | 19 | 10 | 5 | 12.5 | 13.5 | 19 |
| | $\delta$ | 0.5273 $^{(1)}$ | 1.3368 $^{(2)}$ | 1.3416 $^{(3)}$ | 1.3417 $^{(4)}$ | 1.3418 $^{(5)}$ | 0.0437 $^{(1)}$ | 0.2943 $^{(2)}$ | 0.2958 $^{(3)}$ | 0.2988 $^{(4)}$ | 0.3000 $^{(5)}$ |
| 50 | $b$ | 1.1400 $^{(2)}$ | 0.9894 $^{(1)}$ | 1.3421 $^{(5)}$ | 1.3416 $^{(4)}$ | 1.3412 $^{(3)}$ | 0.2830 $^{(2)}$ | 0.0575 $^{(1)}$ | 0.2993 $^{(4.5)}$ | 0.2993 $^{(4.5)}$ | 0.2992 $^{(3)}$ |
| | $\gamma$ | 0.9613 $^{(1)}$ | 3.0143 $^{(2)}$ | 4.0244 $^{(4)}$ | 4.0246 $^{(5)}$ | 3.9731 $^{(3)}$ | 0.3008 $^{(1)}$ | -0.5594 $^{(2)}$ | -0.8999 $^{(4)}$ | -0.9000 $^{(5)}$ | -0.8883 $^{(3)}$ |
| | $\lambda$ | 0.6107 $^{(1)}$ | 1.4651 $^{(2)}$ | 2.4852$^{(3)}$ | 2.4864 $^{(4)}$ | 2.4923 $^{(5)}$ | 0.1480 $^{(1)}$ | -0.1202 $^{(2)}$ | 2.486 $^{(3)}$ | -0.5531 $^{(4)}$ | -0.5555 $^{(5)}$ |
| | $\sum$ranks | 5 | 7 | 15 | 17 | 16 | 5 | 7 | 14.5 | 14.5 | 16 |
| | $\delta$ | 0.3714 $^{(1)}$ | 0.9477 $^{(2)}$ | 0.9487 $^{(3)}$ | 0.9490 $^{(5)}$ | 0.9488 $^{(4)}$ | 0.0553 $^{(1)}$ | 0.2990 $^{(2)}$ | 0.2995 $^{(3)}$ | 0.2997 $^{(5)}$ | 0.2996 $^{(4)}$ |
| 100 | $b$ | 0.4519 $^{(1)}$ | 0.8163 $^{(2)}$ | 0.9487 $^{(4)}$ | 0.9487 $^{(4)}$ | 0.9487 $^{(4)}$ | 0.1274 $^{(1)}$ | 0.1688 $^{(2)}$ | 0.2999 $^{(4)}$ | 0.2999 $^{(4)}$ | 0.2999 $^{(4)}$ |
| | $\gamma$ | 0.5165 $^{(1)}$ | 2.5256 $^{(2)}$ | 2.8460 $^{(4)}$ | 2.8462 $^{(5)}$ | 2.8036 $^{(3)}$ | 0.1524 $^{(1)}$ | -0.7459 $^{(2)}$ | -0.8965 $^{(4)}$ | -0.8997 $^{(5)}$ | -0.8865 $^{(3)}$ |
| | $\lambda$ | 0.4316 $^{(1)}$ | 1.4039 $^{(2)}$ | 1.7483 $^{(3)}$ | 1.7601$^{(4)}$ | 1.7726 $^{(5)}$ | 0.0764 $^{(1)}$ | -0.3197 $^{(2)}$ | -0.5514 $^{(3)}$ | -0.5552 $^{(4)}$ | -0.5596 $^{(5)}$ |
| | $\sum$ranks | 4 | 8 | 14 | 18 | 16 | 4 | 8 | 14 | 18 | 16 |
| | $\delta$ | 0.2512 $^{(1)}$ | 0.6708 $^{(2)}$ | 0.6718 $^{(3)}$ | 0.6737 $^{(5)}$ | 0.6722$^{(4)}$ | 0.0344 $^{(1)}$ | 0.2989 $^{(2)}$ | 0.2991 $^{(3)}$ | 0.2999 $^{(5)}$ | 0.2998 $^{(4)}$ |
| 200 | $b$ | 0.3482 $^{(1)}$ | 0.6547 $^{(2)}$ | 0.6669 $^{(3)}$ | 0.6778 $^{(5)}$ | 0.6771 $^{(4)}$ | 0.1279 $^{(1)}$ | 0.2773 $^{(2)}$ | 0.2881 $^{(3)}$ | 0.2993 $^{(4)}$ | 0.2998 $^{(5)}$ |
| | $\gamma$ | 0.3711 $^{(1)}$ | 1.9821 $^{(2)}$ | 2.0125 $^{(3.5)}$ | 2.0125 $^{(3.5)}$ | 1.9818 $^{(5)}$ | 0.0911 $^{(1)}$ | -0.8814 $^{(2)}$ | -0.8999 $^{(4.5)}$ | -0.8999 $^{(4.5)}$ | -0.8862 $^{(3)}$ |
| | $\lambda$ | 0.3001 $^{(1)}$ | 1.1754 $^{(2)}$ | 1.2384 $^{(3)}$ | 1.2442 $^{(4)}$ | 1.2544 $^{(5)}$ | -0.0008 $^{(1)}$ | -0.4967 $^{(2)}$ | -0.5531 $^{(3)}$ | 0.5557 $^{(4)}$ | -0.5605 $^{(5)}$ |
| | $\sum$ranks | 4 | 8 | 12.5 | 17.5 | 18 | 4 | 8 | 13.5 | 13.5 | 17 |
| | $\delta$ | 0.2178 $^{(1)}$ | 0.4743 $^{(4)}$ | 0.4743 $^{(4)}$ | 0.4743 $^{(4)}$ | 0.4741 $^{(2)}$ | 0.0597 $^{(1)}$ | 0.2997 $^{(2)}$ | 0.2999 $^{(3)}$ | 0.3000 $^{(4.5)}$ | 0.3000 $^{(4.5)}$ |
| 400 | $b$ | 0.3159 $^{(1)}$ | 0.4740 $^{(2)}$ | 0.4783 $^{(5)}$ | 0.4743 $^{(3.5)}$ | 0.4743 $^{(3.5)}$ | 0.1538 $^{(1)}$ | 0.2995 $^{(2)}$ | 0.2996 $^{(3)}$ | 0.2999 $^{(5)}$ | 0.2998 $^{(4)}$ |
| | $\gamma$ | 0.3449 $^{(1)}$ | 1.4198 $^{(3)}$ | 1.4230 $^{(4.5)}$ | 1.4230 $^{(4.5)}$ | 1.4006 $^{(2)}$ | 0.1108 $^{(1)}$ | -0.8979 $^{(3)}$ | -0.8998 $^{(4)}$ | -0.8999 $^{(5)}$ | -0.8857 $^{(2)}$ |
| | $\lambda$ | 0.2593 $^{(1)}$ | 0.8610 $^{(2)}$ | 0.8781 $^{(4)}$ | 0.8756 $^{(3)}$ | 0.8847 $^{(5)}$ | -0.0558 $^{(1)}$ | -0.5382 $^{(2)}$ | -0.5549 $^{(4)}$ | -0.5533 $^{(3)}$ | -0.5592 $^{(5)}$ |
| | $\sum$ranks | 4 | 11 | 17.5 | 15 | 12.5 | 4 | 9 | 14 | 17.5 | 15.5 |
| | $\delta$ | 0.1661 $^{(1)}$ | 0.3354 $^{(3.5)}$ | 0.3354 $^{(3.5)}$ | 0.3354 $^{(3.5)}$ | 0.3354 $^{(3.5)}$ | 0.0546 $^{(1)}$ | 0.3000 $^{(3.5)}$ | 0.3000 $^{(3.5)}$ | 0.3000 $^{(3.5)}$ | 0.3000 $^{(3.5)}$ |
| 800 | $b$ | 0.2644 $^{(1)}$ | 0.3354 $^{(3.5)}$ | 0.3354 $^{(3.5)}$ | 0.3354 $^{(3.5)}$ | 0.3354 $^{(3.5)}$ | 0.1404 $^{(1)}$ | 0.3000 $^{(3.5)}$ | 0.3000 $^{(3.5)}$ | 0.3000 $^{(3.5)}$ | 0.3000 $^{(3.5)}$ |
| | $\gamma$ | 0.3155 $^{(1)}$ | 1.0050 $^{(3)}$ | 1.0062 $^{(4.5)}$ | 1.0062 $^{(4.5)}$ | 0.9881 $^{(2)}$ | 0.0996 $^{(1)}$ | -0.8989 $^{(3)}$ | -0.9000 $^{(4.5)}$ | -0.9000 $^{(4.5)}$ | -0.8836 $^{(2)}$ |
| | $\lambda$ | 0.2402 $^{(1)}$ | 0.6168 $^{(2)}$ | 0.6217 $^{(4)}$ | 0.6204 $^{(3)}$ | 0.6246 $^{(5)}$ | -0.0646 $^{(1)}$ | -0.5474 $^{(2)}$ | -.05557 $^{(4)}$ | -0.5546 $^{(3)}$ | -0.5585 $^{(5)}$ |
| | $\sum$ranks | 4 | 12 | 15.5 | 14.5 | 14 | 4 | 12 | 15.5 | 14.5 | 14 |

Tables [5.3] and [5.4] illustrate that the Abias exhibits a decline with increase in sample size. Furthermore, for all estimation methods, increasing the sample size leads to a reduction in RMSE. The results underscore the robustness of the TLMOGom-W distribution, evident in the values of RMSE across model parameters.

Table 4. **Rankings of Estimation Techniques for the TLMOGom-W FoD: Partial and Overall Ranks**

| Parameters | $m$ | MLE | WLS | LS | CVM | AD |
|---|---|---|---|---|---|---|
| | 25 | 18 $^{(2)}$ | 12 $^{(1)}$ | 24 $^{(3)}$ | 28 $^{(4)}$ | 38 $^{(5)}$ |
| | 50 | 10 $^{(1)}$ | 14 $^{(2)}$ | 29.5 $^{(3)}$ | 31.5 $^{(4)}$ | 32 $^{(5)}$ |
| $\delta = 0.7, b = 0.7, \gamma = 0.9, \lambda = 0.9$ | 100 | 8 $^{(1)}$ | 16 $^{(2)}$ | 28 $^{(3)}$ | 36 $^{(5)}$ | 32 $^{(4)}$ |
| | 200 | 8 $^{(1)}$ | 16 $^{(2)}$ | 26 $^{(3)}$ | 31 $^{(4)}$ | 35 $^{(5)}$ |
| | 400 | 8 $^{(1)}$ | 20 $^{(2)}$ | 35 $^{(5)}$ | 32.5 $^{(4)}$ | 28 $^{(3)}$ |
| | 800 | 8 $^{(1)}$ | 24 $^{(2)}$ | 31 $^{(5)}$ | 29 $^{(4)}$ | 28 $^{(3)}$ |
| $\sum$ranks | | 7 | 11 | 22 | 25 | 25 |
| Overall rank | | 1 | 2 | 3 | 4.5 | 4.5 |

Figures [5.1] and [5.2] illustrate the reduction in RMSE of the parameters as the sample size increases for each estimation method. For larger sample sizes, all the methods of estimation yielded good estimates.

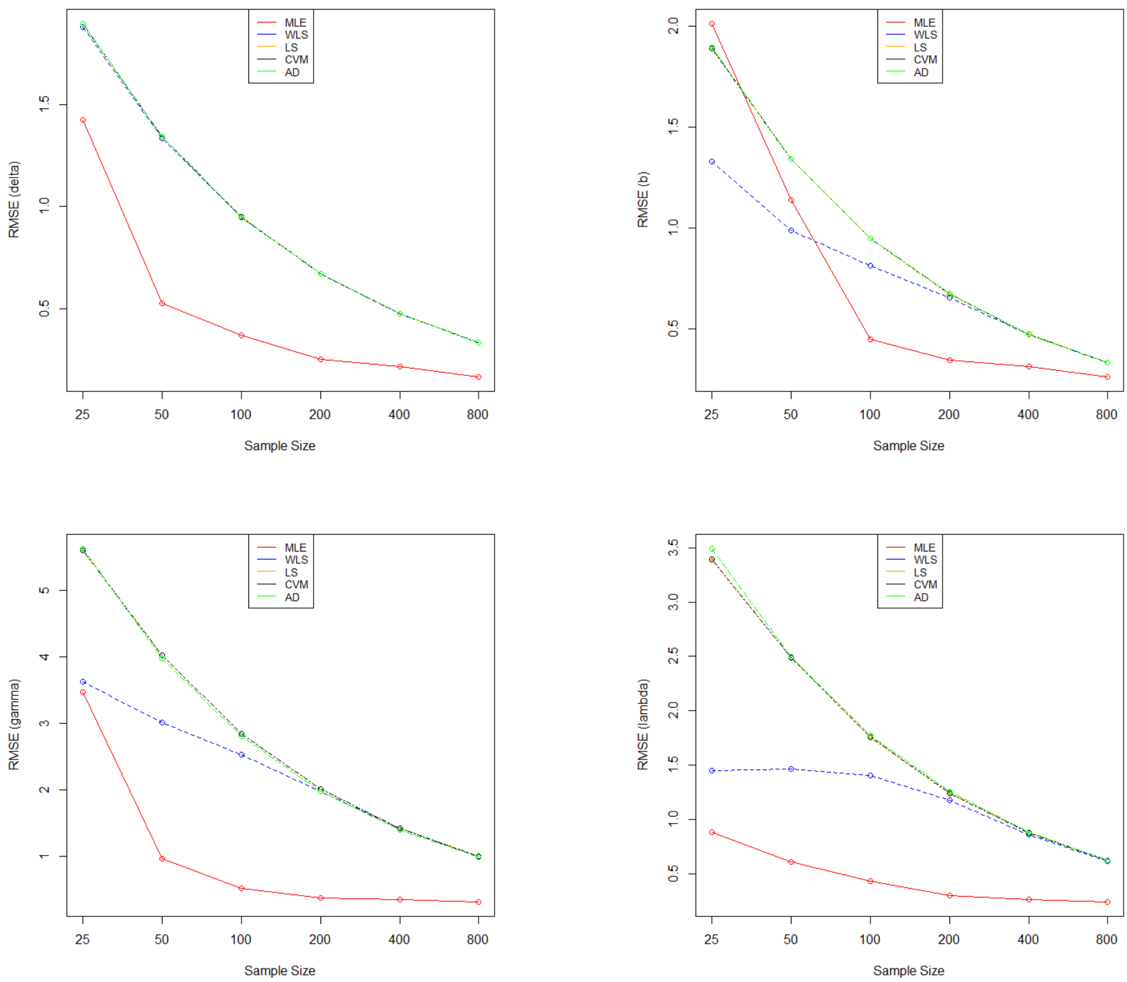


Figure 8. TLMOGom-W RMSE Plots

## 6. Applications

The TLMOGom-W distribution, a special case of the TLMOGom-G is applied to real-life datasets to examine the utility and applicability of the proposed FoD. The analysis incorporates both complete and censored datasets, all of which are presented in the Appendix section. To assess the model appropriateness we employ several goodness-of-fit test statistics including: -2LogLikelihood ($-2ln(L)$), Akaike Information Criterion (AIC), Consistent Akaike Information Criterion (CAIC), Bayesian Information Criterion (BIC), Cramer-von-Mises (CVM), Anderson-Darling (AD), Kolmogorov-Smirnov (K-S) and its p-value. The model that consistently ranks lowest across test statistics is considered the best. If some models have fewer parameters than the TLMOGom-W model, BIC is often prioritized. A higher p-value (typically greater than 0.05) suggests the model is an acceptable fit. Thus the model with the highest p-value is considered the best. Their associated mathematical definitions can be accessed in the **web appendix**.

Several different equi-parameter models were included in the comparisons. The models are: The Topp-Leone odd Burr III log-logistic (TLOBIIILLo) by Moakofi et al. [28], the exponential Lindley odd log-logistic Weibull (ELOLLW) by Korkmaz et al. [23], exponentiated Weibull exponential (EWE) by Elgarhy et al. [19], Marshall-Olkin extended Weibull (MOEW) by Ahmad et al. [3], Marshall-Olkin Gompertz-Weibull (MOGomW) by Chipepa and Oluyede [13], and odd exponentiated half logistic Burr XII (OEHLBXII) by Aldahlan and Afify [4]. The pdfs of these distributions are given in the appendix. A comparison of the $TLMOGom-W$ and its nested models was also conducted via the likelihood ratio tests.

### 6.1. *Bladder Cancer Data*

The first dataset pertains to the remission times of 128 patients afflicted with bladder cancer and was analyzed by Lee and Wang [25] and Klakattawi [22]. The remission times, measured in months, are given in the **web appendix**.

Table 5. **Estimates and Statistics**

| | Estimates | | | | Statistics | | | | | | | |
|---|---|---|---|---|---|---|---|---|---|---|---|---|
| Distribution | $\delta$ | $b$ | $\gamma$ | $\lambda$ | $-2ln(L)$ | AIC | CAIC | BIC | $CVM$ | $AD$ | K−S | p−value |
| TLMOGom-W | $5.5705\times10^{3}$ | 1.9777 | 3.0685 | 383.1700 | 819.2923 | 827.2925 | 827.6177 | 838.7006 | 0.0196 | 0.1261 | 0.0342 | 0.9983 |
| | $(1.3446\times10^{-5})$ | (0.5829) | (0.0914) | (0.0060) | | | | | | | | |
| TLMOGomW$(\delta,1,1,\lambda)$ | 58.7536 | - | - | 0.1903 | 844.9552 | 848.9552 | 849.0512 | 854.6593 | 0.3433 | 2.0307 | 0.1036 | 0.1284 |
| | (9.5478) | (-) | (-) | (0.0067) | | | | | | | | |
| TLMOGom-W$(1,b,\gamma,\lambda)$ | - | 29.0874 | 0.3125 | 0.2242 | 830.1083 | 836.1083 | 836.3018 | 844.6644 | 0.1243 | 0.8363 | 0.0692 | 0.5715 |
| | (-) | (10.3129) | (0.2636) | (0.0561) | | | | | | | | |
| TLMOGom-W$(\delta,1,\gamma,\lambda)$ | 11.1230 | - | $6.9433\times10^{-9}$ | 0.4043 | 863.0305 | 869.0293 | 869.2228 | 877.5854 | 0.1201 | 0.7095 | 0.2502 | $2.1910\times10^{-7}$ |
| | (1.2634) | (-) | (0.0243) | (0.0202) | | | | | | | | |
| TLMOGomW$(\delta,b,1,\lambda)$ | 8.5671 | 5.1239 | - | 0.1566 | 827.0467 | 833.0467 | 833.2403 | 844.6028 | 0.0306 | 0.1975 | 0.0390 | 0.9199 |
| | (3.6520) | (2.2260) | (-) | (0.0102) | | | | | | | | |
| TLMOGom-W$(1,b,1,\lambda)$ | - | 88.9219 | - | 0.1220 | 834.7284 | 838.7284 | 838.8244 | 844.4325 | 0.1727 | 1.1435 | 0.0791 | 0.4000 |
| | (-) | (8.4528) | (-) | (0.0057) | | | | | | | | |
| | $\alpha$ | $\beta$ | $b$ | $\lambda$ | | | | | | | | |
| TLOBIIILLo | 11.3701 | 11.0852 | 0.4222 | 0.0763 | 838.1635 | 846.1635 | 846.4887 | 857.5716 | 0.2082 | 1.3743 | 0.0829 | 0.3426 |
| | (0.0181) | (16.9920) | (0.2289) | (0.0466) | | | | | | | | |
| | $\alpha$ | $\beta$ | $\lambda$ | $k$ | | | | | | | | |
| MOEW | 1.0558 | 0.0031 | 0.1099 | 0.04235 | 828.6523 | 836.6523 | 836.9775 | 848.0605 | 0.1254 | 0.7510 | 0.0811 | 0.3685 |
| | (0.3217) | $(3.4925\times10^{-10})$ | (0.0199) | (0.1599) | | | | | | | | |
| | $\delta$ | $\theta$ | $\lambda$ | $\gamma$ | | | | | | | | |
| MOGomW | 0.3134 | 0.0313 | 1.1935 | $2.9347\times10^{-10}$ | 825.7899 | 833.7899 | 834.1145 | 845.1974 | 0.0526 | 0.3415 | 0.0843 | 0.3236 |
| | (0.2689) | (0.0301) | (0.1489) | $(6.7012\times10^{-3})$ | | | | | | | | |
| | $\beta$ | $\lambda$ | $\theta$ | $\gamma$ | | | | | | | | |
| ELOLLW | 124.7271 | 6.1802 | 0.1147 | 0.7257 | 822.7913 | 830.7913 | 831.1165 | 842.1994 | 0.0666 | 0.4118 | 0.0535 | 0.8568 |
| | (0.0271) | (7.5861) | (0.3219) | (0.0076) | | | | | | | | |
| | $\alpha$ | $\lambda$ | $\beta$ | $a$ | | | | | | | | |
| EWE | 1.7511 | 0.0361 | 0.7008 | 1.1147 | 852.3037 | 860.3037 | 860.6289 | 871.7119 | 0.3207 | 1.9091 | 0.1283 | 0.0955 |
| | (0.3588) | (0.0066) | (0.0861) | ( 0.2327) | | | | | | | | |
| | $a$ | $b$ | $\alpha$ | $\beta$ | | | | | | | | |
| OEHLBXII | 0.3925 | 0.0274 | .6829 | 0.3660 | 881.8121 | 889.8121 | 890.1373 | 901.2202 | 0.3274 | 1.9125 | 0.1166 | 0.1116 |
| | (0.0649) | (0.0187) | (1.0211) | (0.0976) | | | | | | | | |

Analysis of the goodness-of-fit statistics shows that the TLMOGom-W performed better than all the six (6) competing models. The profile plots in Figure 9 reveal that the TLMOGom-W model parameters on bladder cancer data can be uniquely identified.

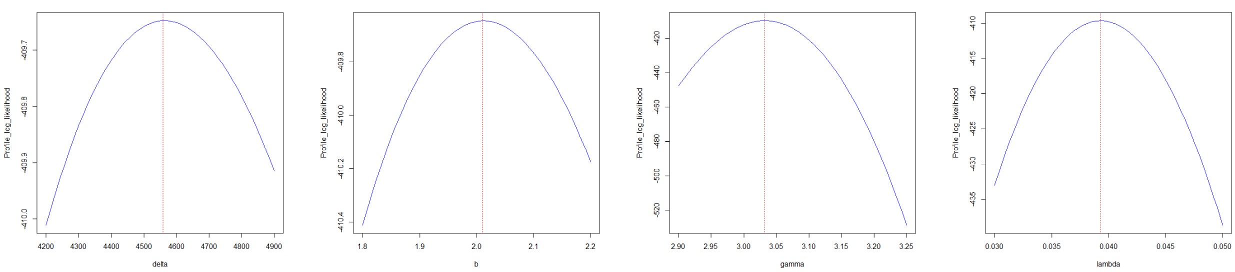


(a) (b) (c) (d)

Figure 9. Profile log-likelihood plots showing TLMOGOM-W parameters on bladder cancer data

The estimated variance-covariance matrix is given as:

$$\begin{bmatrix} 1.8079\times10^{-10} & 7.8178\times10^{-6} & 1.1288\times10^{-6} & -6.8882\times10^{-8} \\ 7.8178\times10^{-6} & 0.3398 & 0.0503 & -3.0979\times10^{-3} \\ 1.1288\times10^{-6} & 0.0503 & 8.3530\times10^{-3} & -5.3333\times10^{-4} \\ -6.8882\times10^{-8} & -3.0979\times10^{-3} & -5.3333\times10^{-4} & 3.6218\times10^{-5} \end{bmatrix}.$$

The approximate $95\%$ two-sided confidence intervals (CIs) are given as: $\delta \in [5.5705 \times 10^3 \pm 2.6354 \times 10^{-5}]$, $b \in [1.9777 \pm 1.1425]$, $\gamma \in [3.0685 \pm 0.1791]$ and $\lambda \in [383.1700 \pm 0.0118]$, confirming statistical significance of model parameters.

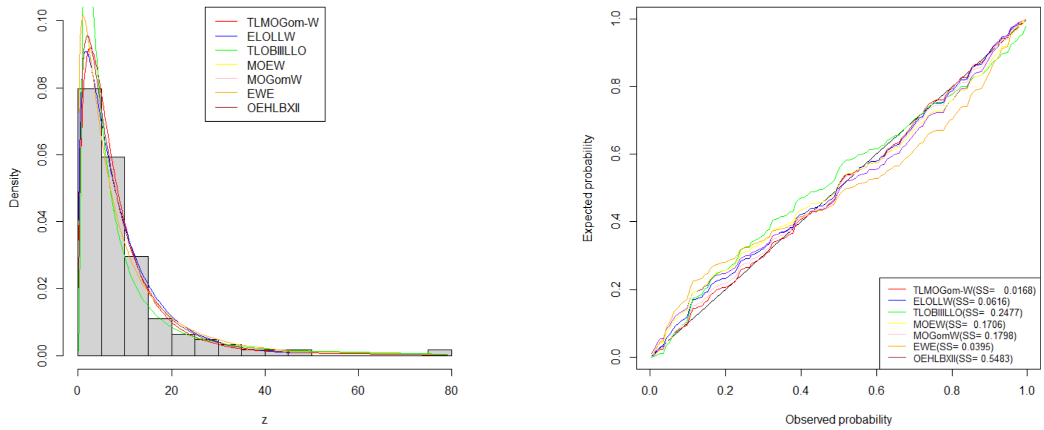


(a) (b)

Figure 10. Densities Plots and PP plots for bladder cancer

Analysis of Figure [6.1] shows that the TLMOGom-W model fits bladder cancer data better than the competing models since it has a smaller value for the SS statistic.

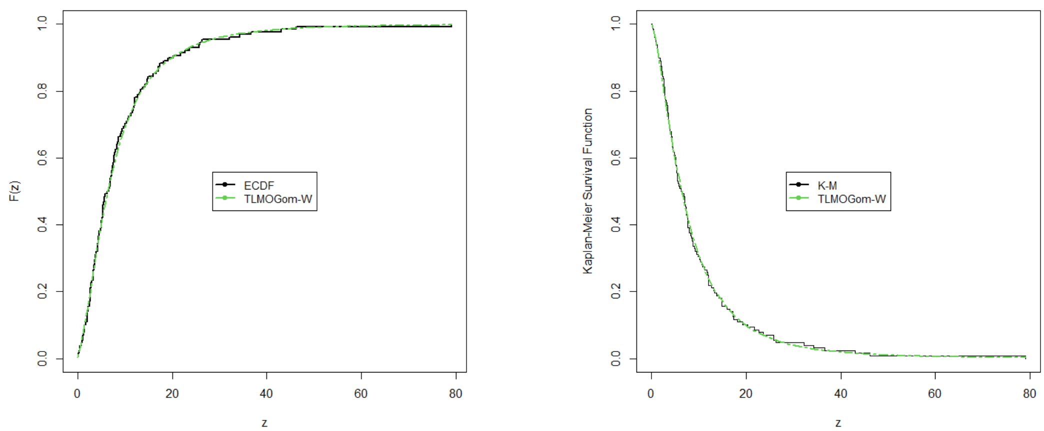


(a) (b)

Figure 11. Fitted ECDF curve and K-M survival plots for bladder cancer data

Figure [6.2] shows empirical cdf and fitted cdf and K-M survival curves for bladder cancer data. There is near perfect coincidence between the observed and fitted suggesting that the TLMOGom-W model is very good fit to bladder cancer data. Figure [6.3] depicts that the hrf has an upside down bathtub shape.

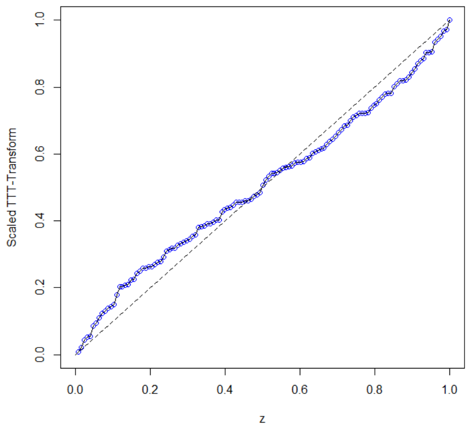


(a)

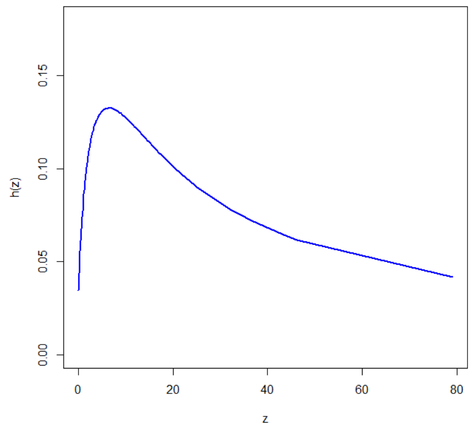


(b)

Figure 12. Fitted TTT scaled and hrf plots for bladder cancer data

### *6.2. Censored Bladder Cancer Data*

The second dataset, which is censored, consists of the remission times (in months) of a randomly selected sample of 137 bladder cancer patients, as cited in the paper by Lee and Wang [25]. The censored data are provided in the **web appendix**.

Table 6. **Estimates and Statistics**

| | Estimates | | | | Statistics | | | | |
|---|---|---|---|---|---|---|---|---|---|
| Distribution | $\delta$ | $b$ | $\gamma$ | $\lambda$ | $-2ln(L)$ | AIC | CAIC | BIC | SS |
| TLMOGom-W | $2.8637\times10^{3}$ | 2.1481 | 2.9470 | 4.0768 | 836.6893 | 844.6893 | 844.9923 | 847.3729 | 0.0731 |
| | $(3.6165\times10^{-5})$ | (0.6438) | (0.0989) | $(6.6029\times10^{-3})$ | | | | | |
| TLMOGom-W$(\delta, 1, 1, \lambda)$ | 29.8242 | - | - | 0.2188 | 847.1655 | 853.1655 | 853.3460 | 868.1059 | 0.1048 |
| | (10.7165) | (-) | (-) | (0.0555) | | | | | |
| TLMOGom-W$(\delta, 1, \gamma, \lambda)$ | $1.2901\times10^{8}$ | - | 4.1728 | 0.0181 | 840.9228 | 846.9228 | 847.1033 | 855.6827 | 0.1035 |
| | $(1.1880\times10^{-11})$ | (-) | (0.0185) | $(1.8110\times10^{-3})$ | | | | | |
| TLMOGomW$(1, b, \gamma, \lambda)$ | - | 21.3430 | $1.3305\times10^{-8}$ | 0.4438 | 856.6610 | 862.6610 | 862.8415 | 871.4209 | 0.3178 |
| | (-) | (3.1682) | (0.0361) | (0.0298) | | | | | |
| TLMOGomW$(\delta, b, 1, \lambda)$ | 57.3564 | 16.5841 | - | 0.0150 | 845.6701 | 851.6701 | 851.8426 | 856.9522 | 0.2651 |
| | (7.1030) | (1.2284) | (-) | (0.0111) | | | | | |
| TLMOGom-W$(1, b, 1, \lambda)$ | - | 91.2669 | - | 0.1189 | 851.6309 | 855.6309 | 855.7802 | 861.4709 | 0.1480 |
| | (-) | (8.4822) | (-) | (0.0056) | | | | | |
| | $\alpha$ | $\beta$ | $b$ | $\lambda$ | | | | | |
| TLOBIIILLo | 0.8180 | 11.0438 | 0.4343 | 1.0317 | 854.7989 | 862.7989 | 863.1019 | 874.4788 | 0.1800 |
| | (1.6787) | (7.4087) | (0.3243) | (2.1173) | | | | | |
| | $\alpha$ | $\beta$ | $\lambda$ | $k$ | | | | | |
| MOEW | $2.7362\times10^{6}$ | 11.6540 | 0.0119 | 0.1105 | 837.2635 | 845.2635 | 845.6785 | 847.7654 | 0.0838 |
| | $(9.8179\times10^{-8})$ | (0.2706) | (0.0220) | (0.0142) | | | | | |
| | $\delta$ | $\theta$ | $\lambda$ | $\gamma$ | | | | | |
| MOGomW | $1.7830\times10^{3}$ | $9.5569\times10^{-3}$ | 0.0261 | 8.3577 | 838.1669 | 846.1669 | 846.4699 | 848.8505 | 0.0905 |
| | $(4.9862\times10^{-5})$ | $(4.6283\times10^{-3})$ | $(2.5299\times10^{-3})$ | (0.5500) | | | | | |
| | $\beta$ | $\lambda$ | $\theta$ | $\gamma$ | | | | | |
| ELOLLW | $9.7330\times10^{-7}$ | 0.1321 | 0.7310 | 1.0536 | 844.8293 | 852.8293 | 853.1323 | 855.5129 | 0.1168 |
| | (0.1072) | (0.0216) | $(3.7039\times10^{-3})$ | (0.0681) | | | | | |
| | $\alpha$ | $\lambda$ | $\beta$ | $a$ | | | | | |
| EWE | 1.1665 | 0.0429 | 0.7070 | 0.8983 | 881.9474 | 889.9474 | 890.2504 | 892.6310 | 0.0913 |
| | (0.2515) | (0.0077) | (0.0831) | ( 0.1559) | | | | | |
| | $\alpha$ | $\lambda$ | $a$ | $b$ | | | | | |
| OEHLBXII | 0.3942 | 0.0223 | 3.6690 | 0.3782 | 897.0698 | 905.0698 | 905.3728 | 907.7534 | 0.7174 |
| | (0.0662) | (0.0162) | (1.0234) | (0.1007) | | | | | |

It is evident from Table [6.2], that the TLMOGom-W model out competes the selected models since it has the least values for all the gof statistics.

The estimated covariance matrix is

$$\begin{bmatrix} 1.3079\times10^{-9} & 2.3242\times10^{-5} & 3.3244\times10^{-6} & -2.0675\times10^{-7} \\ 2.3242\times10^{-5} & 0.4144 & 0.0604 & -3.7861\times10^{-3} \\ 3.3244\times10^{-6} & 0.0604 & 9.7897\times10^{-3} & -6.3468\times10^{-4} \\ -2.0675\times10^{-7} & -3.7861\times10^{-3} & -6.3468\times10^{-4} & 4.3598\times10^{-5} \end{bmatrix}.$$

The confidence intervals for the parameters, presented at an approximate 95% confidence, are provided as follows: $\delta \in [2.8637 \times 10^3 \pm 7.0883 \times 10^{-5}]$, $b \in [2.1481 \pm 1.2618]$, $\gamma \in [2.9470 \pm 0.1938]$ and $\lambda \in [4.0768 \pm 12.9417 \times 10^{-3}]$, respectively.

### 6.3. *Accelerated Life Test Data*

The data are from research done by Adewara et al. [2] on accelerated life test of 59 conductors, see **web appendix**. Electro-migration, which involves the movement of atoms in the conductors of microcircuits, can result in failures within the circuit. These failures are measured in hours, and there are no instances of censored observations.

Table 7. **Estimates and Statistics**

| | Estimates | | | | Statistics | | | | | | | |
|---|---|---|---|---|---|---|---|---|---|---|---|---|
| Distribution | $\delta$ | $b$ | $\gamma$ | $\lambda$ | $-2ln(L)$ | AIC | CAIC | BIC | $CVM$ | $AD$ | K−S | p−value |
| TLMOGom-W | 105.6415 | 3.2768 | 0.4416 | 0.4968 | 222.4527 | 230.4527 | 231.1934 | 238.7628 | 0.02718 | 0.1578 | 0.0571 | 0.9848 |
| | ($3.5408\times10^{-3}$) | (0.6538) | (0.1606) | (0.2154) | | | | | | | | |
| TLMOGom-W($\delta, 1, 1, \lambda$) | 2255.1000 | - | - | 0.3705 | 228.7159 | 232.7159 | 232.9302 | 238.8710 | 0.0963 | 0.5539 | 0.0813 | 0.7999 |
| | ($5.2245\times10^{-8}$) | (-) | (-) | ($4.8994\times10^{-3}$) | | | | | | | | |
| TLMOGom-W($1, b, \gamma, \lambda$) | - | 680.1100 | 0.3602 | 0.4244 | 232.9546 | 238.9546 | 239.391 | 245.1872 | 0.1418 | 0.8638 | 0.1185 | 0.3514 |
| | (-) | ($1.7210\times10^{-4}$) | (0.1761) | (0.0134) | | | | | | | | |
| TLMOGom-W($\delta, 1, \gamma, \lambda$) | $3.5344\times10^{8}$ | - | 2.8850 | 0.0648 | 302.5947 | 308.5944 | 308.9754 | 315.2085 | 0.1766 | 0.9163 | 0.1750 | 0.2496 |
| | ($1.1601\times10^{-10}$) | (-) | (0.1810) | (0.0091) | | | | | | | | |
| TLMOGomW($\delta, b, 1, \lambda$) | 301.7400 | 2.8752 | - | 0.12970 | 249.6793 | 255.6793 | 256.0323 | 262.5093 | 0.1743 | 0.6435 | 0.1270 | 0.3274 |
| | ($2.4597\times10^{-3}$) | (0.4817) | (-) | ($2.3320\times10^{-3}$) | | | | | | | | |
| TLMOGom-W($1, b, 1, \lambda$) | - | 33.2500 | - | 0.0915 | 432.5381 | 436.5381 | 436.7524 | 440.6932 | 0.0630 | 0.3866 | 0.6019 | $7.7720\times10^{-16}$ |
| | (-) | (0.0001) | (-) | (0.0097) | | | | | | | | |
| | $\alpha$ | $\beta$ | $b$ | $\lambda$ | | | | | | | | |
| TLOBIIILLo | 16.2510 | 366.0000 | 0.6968 | 0.1767 | 237.9898 | 245.9898 | 246.7306 | 254.3000 | 0.1951 | 1.1833 | 0.1288 | 0.2587 |
| | ($9.0693\times10^{-5}$) | ($2.8186\times10^{-4}$) | (0.2177) | ($8.3216\times10^{-3}$) | | | | | | | | |
| | $\alpha$ | $\beta$ | $\lambda$ | $k$ | | | | | | | | |
| MOEW | 249.0700 | 0.0135 | 0.7330 | 1.9582 | 227.5762 | 235.5762 | 236.3169 | 243.8863 | 0.0340 | 0.1968 | 0.1162 | 0.3740 |
| | ($9.5255\times10^{-3}$) | (0.0217) | (0.1520) | (1.0321) | | | | | | | | |
| | $\delta$ | $\theta$ | $\lambda$ | $\gamma$ | | | | | | | | |
| MOGomW | 19.0390 | 0.0502 | 2.1096 | $1.7270\times10^{-5}$ | 226.6815 | 234.6815 | 235.4223 | 242.9917 | 0.0812 | 0.4669 | 0.0811 | 0.8024 |
| | ($5.8846\times10^{-3}$) | (0.0501) | (0.6303) | ($8.1386\times10^{-3}$) | | | | | | | | |
| | $\beta$ | $\lambda$ | $\theta$ | $\gamma$ | | | | | | | | |
| ELOLLW | 80.1189 | 0.4804 | 0.0343 | 3.2150 | 223.0490 | 231.0490 | 231.7897 | 239.3592 | 0.0490 | 0.2727 | 0.0778 | 0.8404 |
| | $(9.6910)\times10^{-5}$ | (0.9210) | (0.2111) | (0.3074) | | | | | | | | |
| | $\alpha$ | $\lambda$ | $\beta$ | $a$ | | | | | | | | |
| EWE | 1.0741 | 1.4198 | 0.1304 | 33.0134 | 222.7285 | 230.7285 | 231.4693 | 239.0387 | 0.0339 | 0.1908 | 0.0752 | 0.8677 |
| | (0.1336) | (7.9655) | (0.7294) | (0.2720) | | | | | | | | |
| | $\alpha$ | $\lambda$ | $a$ | $b$ | | | | | | | | |
| EOHLBXII | 0.7341 | $9.3150\times10^{-4}$ | 11.5660 | 0.3029 | 271.6985 | 279.6989 | 280.4396 | 288.0090 | 0.0882 | 0.4955 | 0.1506 | 0.1242 |
| | (0.1413) | ($9.4777\times10^{-4}$) | ($2.7633\times10^{-3}$) | (0.0392) | | | | | | | | |

Analysis of goodness-of-fit statistics demonstrates that the TLMOGom-W model outperforms all six (6) competing models. Additionally, the profile plots presented in Figure 13 indicate that the parameters of the TLMOGom-W model, when applied to accelerated life test data, are uniquely identifiable. This confirms the robustness and reliability of the model for parameter estimation.

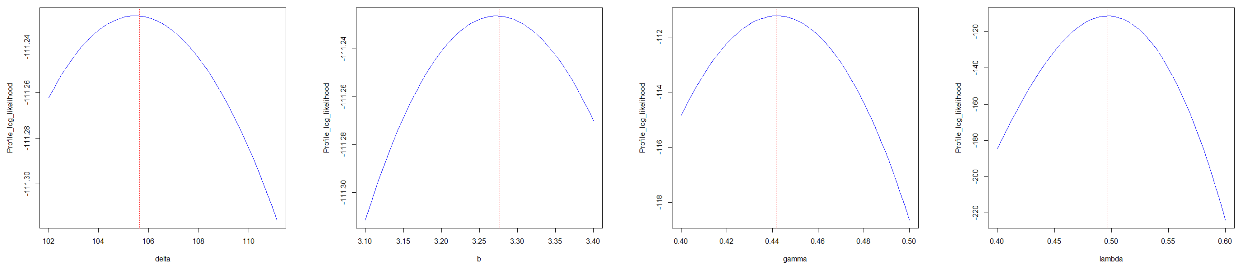


(a) (b) (c) (d)

Figure 13. Profile log-likelihood plots showing TLMOGOM-W parameters on accelerated life test data

The estimated covariance matrix is

$$\begin{bmatrix} 1.2537\times10^{-5} & 0.0023 & \text{-}0.00047 & 0.00051 \\ 0.0023 & 0.4269 & -0.0722 & 0.1021 \\ \text{-}3.5336\times10^{-4} & -0.0722 & 0.0258 & \text{-}0.0345 \\ 0.0005 & 0.1021 & \text{-}0.0345 & 0.0464 \end{bmatrix}.$$

The approximate 95% CIs for the parameters are presented as follows: $\delta \in [105.6415 \pm 6.9400 \times 10^{-3}]$, $b \in [3.2768 \pm 1.2814]$, $\gamma \in [0.4416 \pm 0.3148]$ and $\lambda \in [0.4968 \pm 0.4222]$.

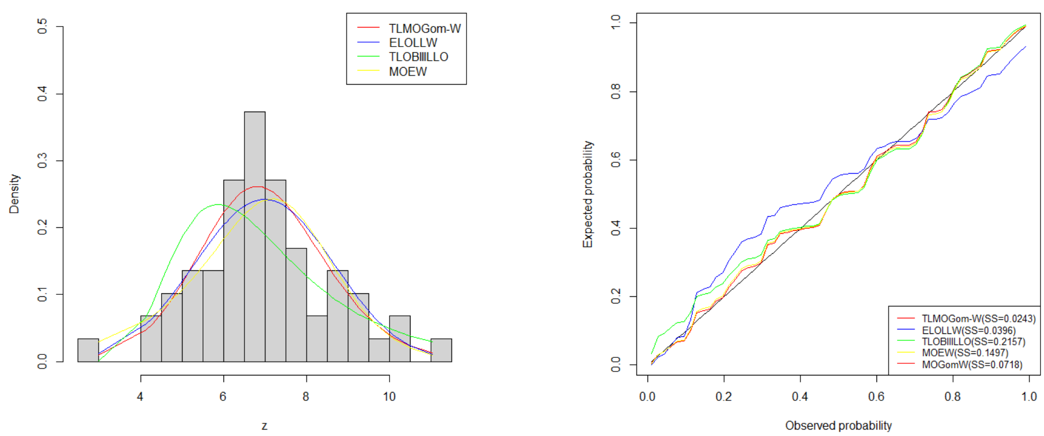


(a) (b)

Figure 14. Densities Plots and PP plots for accelerated life test data

Based on Figure [6.4], it can be concluded that the TLMOGom-W model demonstrates superior data fit compared to the other competing models.

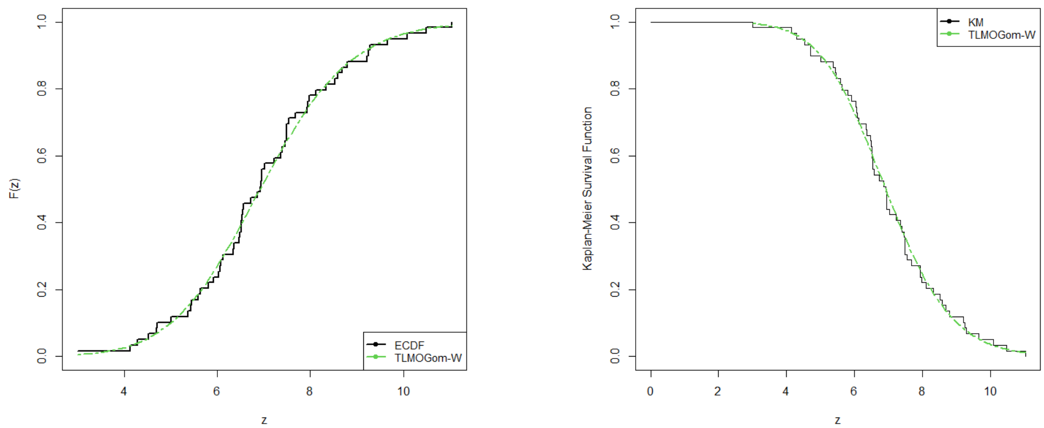


(a) (b)

Figure 15. Fitted ECDF curve and K-M survival plots for accelerated life test Data

Figure 15 shows ECDF and K-M survival curves for accelerated life test data. The TLMOGom-W distribution closely follows the ECDF and K-M survival curves.

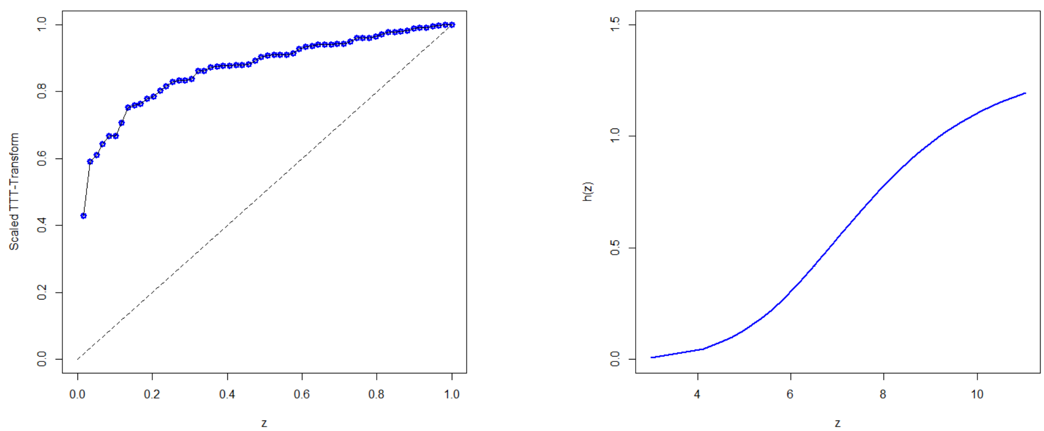


(a) (b)

Figure 16. TTT scaled and hrf plots for Accelerated life test Data

The analysis of the TTT plot and hrf plot in Figure 16 indicates a increasing hazard shape.

### 6.4. *Likelihood Ratio Test Results*

Table [6.4] presents the results of the likelihood ratio test (LRT) which compares the likelihoods of full and nested TLMOGom-W models: one obtained by maximizing the likelihood over the entire parameter space, and the other obtained by imposing a constraint on the parameters. The LRT statistic, computed from $[-2\log(L_{nested}) - (-2\log(L_{fullmodel})]$ follows a $\chi^2_v$, where $v$ are the degrees of freedom (df) corresponding to the parameters difference between the models in comparison. The findings from the LRT confirm that the TLMOGom-W model outperforms the sub-models. This conclusion is supported by the significant chi-square values obtained, indicating that the improvements achieved by the TLMOGom-W model are statistically significant compared to the alternative sub-models.

Table 8. **LRT Results**

| Model | df $v$ | Bladder Cancer $\chi^2(p-value)$ | Censored Bladder Cancer $\chi^2(p-value)$ | Accelerated Life Test $\chi^2(p-value)$ |
|---|---|---|---|---|
| TLMOGom-W$(\delta,1,1,\lambda)$ | 2 | 25.6629($< 0.00001$) | 10.4762(0.0053) | 6.2632( 0.0436) |
| TLMOGom-W$(1,b,\gamma,\lambda)$ | 1 | 10.8160(0.0010) | 19.9717($< 0.00001$) | 10.5019(0.0012) |
| TLMOGom-W$(\delta,1,\gamma,\lambda)$ | 1 | 43.7382($< 0.00001$) | 4.2335(0.0396) | 80.1420($< 0.00001$) |
| TLMOGomW$(\delta,b,1,\lambda)$ | 2 | 9.7544(0.00218) | 9.9808(0.0071) | 27.1266(0.0001) |
| TLMOGom-W$(1,b,1,\lambda)$ | 2 | 15.4361(0.0004) | 14.9416(0.0006) | 210.0854($< 0.00001$) |

## 7. Summary of the Research

In conclusion, a new FoD called the TLMOGom-G FoD was developed. Statistical properties including Rényi entropy, order statistics, stochastic ordering, and moments, were derived. The MLE technique demonstrated superior performance in the estimation of the TLMOGom-W parameters compared to alternative methods such as AD, CVM, LS, and WLS. The consistency of the proposed distribution was confirmed via Monte Carlo simulations. By applying the TLMOGom-W distribution, a special case of the FoD to real-world data sets including bladder cancer, censored bladder cancer, and accelerated life test, it was evident that the TLMOGom-W outperformed other competing models. This highlights the practical significance and improved goodness-of-fit provided by the TLMOGom-W distribution in modelling these specific data sets.

Based on the findings regarding the TLMOGom-G FoD, it is recommended to explore Bayesian methods to enhance parameter estimation and uncertainty quantification in future applications. Implementing Bayesian frameworks could provide more robust inference, particularly in cases with limited data. Additionally, employing bivariate extensions of the TLMOGom-G FoD may yield deeper insights into the relationships between multiple variables in real-world datasets. This dual approach could further strengthen the model's applicability and performance across diverse statistical scenarios.

### *Appendix*

https://drive.google.com/file/d/1AgGpCMVC8bW9CtDsjb8jB3_5bPMa-h3q/view?usp=sharing

REFERENCES


1. Abdullah, Z.M., Hussain, N.K., Fawzi, F.A., Abdal-Hammed, M.K. and Khaleel, M.A., *Estimating Parameters of Marshall-Olkin Topp-Leon Exponential Distribution via Grey Wolf Optimization and Conjugate Gradient with Application*, International Journal of Nonlinear Analysis and Applications, vol. 13, no. 1, pp. 3491-3503, 2022.
2. Adewara, J. A., Adeye, J. S., Mundher, A. K., and Aako, O. L., *Exponentiated Gompertz Exponential Distribution: Derivation, Properties and Applications*, Journal of the Turkish Statistical Association, vol. 13, no. 1, pp. 12-28, 2021.
3. Ahmad, H. H., Bdair, O. M. and Ahsanullah, M. A., *On Marshall-Olkin Extended Weibull Distribution*, Journal of Statistical Theory and Applications, vol. 16, no. 1, pp. 1-17, 2017.
4. Aldahlan, M. and Afify, A. Z., *The Odd Exponentiated Half-Logistic Burr XII Distribution*, Pakistan Journal of Statistics and Operation Research, vol. 14, no. 2, pp. 317-329, 2018.
5. Alizadeh, M., Benkhelifa, L., Rasekhi, M. and Husseini, B., *The Odd Log -Logistic Generalised Gompertz Distribution: Properties, Applications and Different Methods of Estimation*, Communications in Mathematics and Statistics, vol. 8, no. 1, pp. 295- 317, 2020.
6. Alsultan, R., *The Marshall-Olkin Pranav Distribution: Theory and Applications*, Pakistan Journal of Statistics and Operation Research, vol. 19, no. 1, pp. 155-166, 2023.

7. Atchadé, M.N., N'bouké, M.A.G., Djibril, A.M., Mutairi, A.A., Mustafa, M.S., Hussam, E., Alsuhabi, H. and Nassr, S.G., *A new Topp-Leone Kumaraswamy Marshall-Olkin Generated Family of Distributions with Applications*, Heliyon, vol. 10, no. 2, pp. e24001. doi: 10.1016/j.heliyon.2024.e24001, 2024.
8. Barreto-Souza, W. and Bakouch, H. S., *A New Lifetime Model with Decreasing Failure Rate*, Statistics, vol. 47, no. 6, pp. 465-476, 2013.
9. Barreto-Souza, W., Lemonte, J. A. and Cordeiro, G. M., *General Results for the Marshall and Olkin's Family of Distributions*, Anais da Academia Brasileira de Ciencias, vol. 85, no. 2.3, pp. 3-21, 2013.
10. Bourguignon, M., Silva, R. B. and Cordeiro, G. M., *The Weibull-G Family of Probability Distributions*, Journal of Data Science, vol. 12, pp. 53-68, 2014.
11. Brito, E., Cordeiro, G. M., Yousof, H. M., Alizadeh, M. and Silva, G. O., *The Topp-Leone Odd Log Logistic Family of Distributions*, Journal of Statistical Computation and Simulation, vol. 8, no. 7, pp. 3040-3058, 2017.
12. Chipepa, F., Oluyede, B. and Mukubate, B., *The Topp-Leone Marshall-Olkin-G Family of Distributions with Applications*, International journal of Statistics and Probability, vol. 9, no. 4, pp. 1-15, 2020.
13. Chipepa, F. and Oluyede, B., *The Marshall-Olkin-Gompertz-G Family of Distributions: Properties and Applications*, Journal of Nonlinear Sciences and Applications, vol. 14, pp. 250- 267, 2021.
14. Cleaton, J. U. and Lynch, S. D, *Properties of Generalised Log-Logistic Families of Lifetime Distributions*, Journal of Probability and Statistical Science, vol. 4, no. 1, pp. 52-64, 2006.
15. Cordeiro, G. M., Ortega, E. M. M. and Nadarajaah, S., *The Kumaraswamy Weibull Distribution with Application to Failure Data*, Journal of the Franklin Institute, vol. 347, no. 6, pp. 1399-1429, 2010.
16. Cordeiro, G. M., Alizadeh, M., Nascimento, A. D. C. and Rasekhi, M., *The Exponentiated Gompertz Generated Family of Distributions: Properties and Applications*, Chilean Journal of Statistics, vol. 7, no. 1, pp. 51-83, 2016.
17. Ehiwario, J.C., Igabari, J.N. and Ezimadu, P.E, *The Alpha Power Topp-Leone Distribution: Properties, Simulations and Applications*, Journal of Applied Mathematics and Physics, vol. 11, no. 1, pp. 316-331, 2023.
18. El-Gohary, A., Alshamrani, A. and Al-Otaili, A., *The Generalized Gompertz Distribution*, Applied Mathematical Modelling, vol. 37, pp. 13-24, 2013.
19. Elgarhy, M., Shakil, M. and Golam Kibria, B. M., *Exponentiated Weibull-Exponential Distribution with Applications*, Applications and Applied Mathematics: An International Journal, vol. 12, no. 2, pp. 710-72, 2017.
20. Hassan, E.A.A., Elgarhy, M., Eldessouky, E.A, Hassan, O.H.M., Amin, E.A and Almetwally, E.M., *Different Estimation Methods for New Probability Distribution Approach Based on Environmental and Medical Data*, Axioms, vol. 12, no. 2, pp. 51-83, 2023.
21. Jafari, A. A., Tahmasebi, S. and Alizadeh, M., *The Beta Gompertz Distribution*, Revista Colombiana de Estadística, vol. 37, no. 1, pp. 141-158, 2014.
22. Klakattawi, H.S., *Survival Analysis of Cancer Patients Using a New Extended Weibull Distribution*, PLoS ONE, vol. 17, no. 2, pp. 26-42, 2022.
23. Korkmaz, M.C., Yousof, H.M. and Hamedani, G.G., *The Exponential Lindley Odd Log-Logistic-G Family: Properties, Characterizations and Applications*, Journal of Statistical Theory and Applications, vol. 17, no. 3, pp. 554 - 571, 2018.
24. Lawless, J. F., *Statistical Models and Methods for Lifetime Data*, $2^{nd}$ edition, John Wiley and Sons, New Jersey, 2003.
25. Lee, E.T. and Wang, J., *Statistical Methods for Survival Data Analysis*, John Wiley & Sons, Incorporated, pp. DOI:10.1002/0471458546, 2003.
26. Lewis P.A.W., *Distribution of the Anderson-Darling Statistic*, The Annals of Mathematical Statistics, vol. 32, no. 4, pp. 1118-1124, 1961.
27. Marshall, W. A. and Olkin, I., *A new Method for Adding a Parameter in a Family of Distributions with Applications to the Exponentiated and Weibull families*, Biometrika, vol. 84, pp. 641-652, 1997.
28. Moakofi, T., Oluyede, B. and Gabanakgosi, M., *The Topp-Leone Odd Burr III-G Family of Distributions: Model, Properties and Applications*, Journal of Statistics, Optimization and Information Computing, vol. 10, pp. 236-262, 2022.
29. Nasiru, S. and Abubakari, A.G., *Marshall-Olkin Zubair-G Family of Distributions*, Pakistan Journal of Statistics and Operation Research, vol. 18, no. 1, pp. 195-210, 2022.
30. Nkomo, W., Oluyede, B., and Chipepa, F., *Topp-Leone Type I Heavy-Tailed - G Power Series Class of Distributions: Properties, Risk Measures, and Applications*, Statistics, Optimization and Information Computing, vol. 13, no. 1, pp. 88-110, 2025.
31. Oluyede, B., Chamunorwa, S., Chipepa, F. and Alizadeh, M., *TThe Topp-Leone Gompertz-G Family of Distributions with Applications*, Journal of Statistics and Management Systems, vol. 25, no. 6, pp. 1399-1423, 2022.
32. Opone, F. C. and Osemwenkhae, J. E., *The Transmuted Marshall-Olkin Extended Topp-Leone Distribution*, Earthline Journal of Mathematical Sciences, vol. 9, no. 2, pp. 179-199, 2022.
33. Osi, A.A., Doguwa, S.I., Abubakar, Y., Zakari, Y. and Abubakar, U., *Development of Exponentiated Cosine Topp-Leone Generalized Family of Distributions and its Applications to Lifetime Data*, UMYU Scientifica, vol. 3, no. 1, pp. 157-167, 2024.
34. Rényi, A., *On Measures of Entropy and Information*, Proceedings of the Fourth Berkeley Symposium on Mathematical Statistics and Probability, vol. 4, no. 1, pp. 547-561, 1960.
35. Shaked, M. and Shanthikumar, J.G., *Stochastic Orders*, Springer Science and Business Media, pp. 3 - 473, 2007.
36. Sangsanit, Y. and Bodhisuwan, W., *The Topp-Leone Generator of Distributions: Properties and Inferences*, Songklanakarin Journal of Science and Technology, vol. 38, no. 5, pp. 537-548, 2016.
37. Shannon, C. E., *Prediction and Entropy of Printed English*, The Bell System Technical Journal, vol. 30, no. 1, pp. 50-64, 1951.
38. Swain, J.J., Venkatraman, S. and Wilson, J.R., *Least-Squares Estimation of Distribution Functions in Johnson's Translation System*, Journal of Statistical Computation and Simulation, vol. 29, no. 4, pp. 271–297, 1988.
39. William, Q.M. and Escobar, L.A., *Statistical Methods for Reliability Data*, A. Wiley Interscience Publications, pp. 639, 1998.
40. Zografos, K. and Balakrishnan, N., *On Families of Beta and Generalised Gamma Generalised Distributions and Associated Inference*, Statistical Methodology Journal, vol. 6, no. 1, pp.344-362, 2009.